Pharmacokinetic and Pharmacodynamic Modeling of Erythropoiesis Stimulating Agents in Rats

A Thesis

Submitted to the Faculty

of

Drexel University

by

Wendi Chen

in partial fulfillment of the

requirements for the degree

of

Doctor of Philosophy

December 2010

Dedications

To my parents Qingren Chen and Jinxiu Li for their love and support.

Acknowledgments

First and foremost, I would like to express my sincere gratitude to my advisors Drs. Leonid Hrebien and Moshe Kam for their continuous support of my PhD study and research. I appreciate all their contributions of time, ideas, and funding to make my PhD experience productive and stimulating.

I have appreciated the funding and experimental data provided by Centocor Inc. that made my PhD work possible. I gratefully acknowledge Dr. Peter Bugelski, Dr. Ram Achuthanandam and other experts in Centocor Inc.. They show me a whole new world while conducting my research with pharmaceutical data analysis. I appreciate the time that they set aside to discuss my research and provide feedback on my progress. I am grateful to Dr. Sukyung Woo for her kind help in giving me her epoetin-α concentration data.

For this thesis I would like to thank the other two committee members: Drs. Oleh Tretiak and Gail Rosen for their time, interest, and helpful comments.

I would also like to thank my colleagues who have supported me in everything in the lab. Special thanks go to Scott Haney, Pramod Abichandani, Mianyu Wang and Feiyu Xiong.

Last but not the least, I want to thank my entire family for all their spiritual support and encouragement. For my parents who raised me with a love of education and hard work in all my pursuits. For my brothers and sisters who take care of my

parents and let me focus on my studies. And most of all for Yang Huang who believes in, encourages and supports me, even during the tough time in the Ph.D. pursuit.

Table of Contents

List of Tables viii

List of Figures ix

Abstract xii

1. Biological Background 1

1.1 Physiology of Erythropoiesis 1

1.2 Erythropoiesis Stimulating Agents 3

1.2.1 Two commercially available ESAs 3

1.2.2 One newly developed ESA 4

1.2.3 Different biological properties 5

2. Background on Pharmacokinetic and Pharmacodynamic Analysis 6

2.1 Pharmacokinetic Analysis 8

2.1.1 Non-compartmental pharmacokinetic analysis 10

2.1.2 Compartmental pharmacokinetic analysis 12

2.2 Pharmacodynamic Analysis 18

2.2.1 Direct response PD models 18

2.2.2 Indirect response PD models 19

2.2.3 Cell life span PD models 22

2.2.4 *Ad-hoc* response PD models 23

2.3 Original Contributions 24

3. Our Pharmacokinetic/Pharmacodynamic Model 25

3.1 Pharmacokinetic Model 25

3.2 Pharmacodynamic Model 27

3.3 Derivation of Effect Function $E(t)$ 31

4. Evaluation of PK/PD Model Using Biological Data 33

4.1 Agents 33

4.2 Rats 33

4.3 Data Set 34

4.4 Data Analysis 35

4.5 Results 36

4.5.1 PK model results 36

4.5.2 PD model results 42

4.6 Discussion 49

4.7 Conclusion 51

5. An Application of PK/PD modeling: Dose Threshold Study . 53

5.1 Introduction 53

5.2 Experimental Data and Data Analysis 54

5.3 Two Criteria 55

5.4 Results 56

5.5 Discussion 61

6. Summary and Future Work 62

6.1 Summary of Thesis 62

6.2 Future Work 63

Bibliography 64

Appendix A: List of Symbols 70

Appendix B: List of Abbreviations 74

Vita 76

List of Tables

4.1 Non-compartmental analysis for epoetin-α, darbepoetin-α and CNTO 530 39

4.2 Estimated PK parameters for all three ESAs using our model . . . 41

4.3 Estimated PD parameters for all three ESAs using our model . . . 47

5.1 Percentage of RBC counts within the normal range of CNTO 530 . 56

5.2 R^2 calculated from the prediction of drug responses (RET, RBC and HGB) using our model for CNTO 530 61

List of Figures

1.1 The relative sizes and nucleus to cytoplasm ratios of erythroid cells at various stages of erythropoiesis: the color of the cytoplasm describing the relative content of ribosomes (dark blue) and hemoglobin (red) . . . 2

2.1 Relationship between pharmacokinetics and pharmacodynamics . . 6

2.2 PK/PD modeling as combination of two pharmacological processes: pharmacokinetics describing concentration-time courses of drugs and pharmacodynamics describing effect-concentration relationships of drugs . . . 7

2.3 Four processes involved in pharmacokinetics: absorption, distribution, metabolism and excretion (ADME) 9

2.4 A general one-compartmental PK model for i.v. dosing 13

2.5 A general one-compartmental PK model for s.c. dosing 13

2.6 A general two-compartmental PK model for i.v. dosing 14

2.7 A general two-compartmental PK model for s.c. dosing 15

2.8 A one-compartmental PK model for i.v. dosing with Michaelis-Menten elimination 16

2.9 The saturation curve of Michaelis-Menten elimination 17

2.10 Diagram of a typical direct response PD model. It is also a sigmoid E_{max} model 19

2.11 Schematics of four basic indirect response PD models characterized by either inhibition or stimulation of the response variable 21

2.12 Schematic of a typical cell lifespan model 23

3.1 A two-compartmental PK model 26

3.2 A diagram showing our PD model 28

3.3 A diagram of erythropoiesis 29

3.4 The simplified PD model applied to RBC counts for solving E(t) . . 31

4.1 Epoetin-α concentration versus time profile (0.0405 mg/kg) estimated from experimental data provided by Woo et al. (2006) 37

4.2 Darbepoetin-α concentration versus time profile (0.0005 mg/kg) estimated from experimental data provided by Yoshioka et al. (2007) . . . 38

4.3 CNTO 530 concentration versus time profile (0.3 mg/kg) estimated from our PK experiment 38

4.4 Predicted concentration of all three ESAs at a dosage level of 0.3 mg/kg 40

4.5 We implemented the PK/PD model in Woo et al. (2006) at a dose 1350 IU/kg (0.0135 mg/kg) and ran an extended simulation that went to 1728 hours (72 days). A significant inconsistency in the model can be seen in the plots of RET and RBC after 1440 hours (60 days) 42

4.6 The plots of the experimental data (RET, RBC and HGB) and their model predicted curves from our PD model for epoetin-α 43

4.7 The plots of the experimental data (RET, RBC and HGB) and their model predicted curves from our PD model for darbepoetin-α 44

4.8 The plots of the experimental data (RET, RBC and HGB) and their model predicted curves from our PD model for CNTO 530 45

4.9 Goodness-of-fit of RET, RBC and HGB for PD modeling of epoetin-α 46

4.10 Goodness-of-fit of RET, RBC and HGB for PD modeling of darbepoetin-α 46

4.11 Goodness-of-fit of RET, RBC and HGB for PD modeling of CNTO 530 46

4.12 Means and SDs of the normalized estimates of the PD parameters for all three ESAs 48

4.13 E(t) for all three ESAs with dosage 0.1 mg/kg 48

5.1 RET profiles after s.c. administration of CNTO 530 with dosage levels of 0.005 mg/kg, 0.01 mg/kg, 0.02 mg/kg, 0.04 mg/kg, 0.08 mg/kg, 0.16 mg/kg, 0.32 mg/kg, and 1 mg/kg 58

5.2 RBC profiles after s.c. administration of CNTO 530 with dosage levels of 0.005 mg/kg, 0.01 mg/kg, 0.02 mg/kg, 0.04 mg/kg, 0.08 mg/kg, 0.16 mg/kg, 0.32 mg/kg, and 1 mg/kg 59

5.3 HGB profiles after s.c. administration of CNTO 530 with dosage levels of 0.005 mg/kg, 0.01 mg/kg, 0.02 mg/kg, 0.04 mg/kg, 0.08 mg/kg, 0.16 mg/kg, 0.32 mg/kg, and 1 mg/kg 60

5.4 Goodness-of-fit of RET, RBC and HGB for PD model predication of CNTO 530 at 0.08, 0.16, 0.32 and 1 mg/kg 60

Abstract

Pharmacokinetic and Pharmacodynamic Modeling of Erythropoiesis Stimulating Agents in Rats
Wendi Chen
Leonid Hrebien, Ph.D. and Moshe Kam, Ph.D.

Erythropoiesis is a process by which red blood cells are produced in the bone marrow. Disruption of this process can lead to anemia. Erythropoiesis stimulating agents (ESAs), such as epoetin-α and darbepoetin-α, have been developed to treat anemia. CNTO 530 is a novel ESA that has a longer terminal half-life than either epoetin-α or darbepoetin-α. As these ESAs all activate erythropoietin receptor (EPO-R), we hypothesize that any differences in the pharmacologic activity are solely dependent on their pharmacokinetic properties. To test this hypothesis, we proposed a new Pharmacokinetic/Pharmacodynamic (PK/PD) model to account for the pharmacological response. Rats received a single subcutaneous (s.c.) dose of the ESA and reticulocyte (RET) counts, red blood cell (RBC) counts and hemoglobin (HGB) levels were measured for up to 72 days (1728 hours) post-dosing. Various dosage levels were studied for each drug. A new indirect response model with multiple regulatory effects was used to characterize the PD responses and a linear two-compartmental model was used to characterize the PK responses. All three agents caused a dose responsive increase in RET, RBC and HGB. Compared to epoetin-α and darbepoetin-α, CNTO 530 caused a longer-lived increase in these parameters. A single PK/PD model could represent all three agents. However, when comparing among the erythropoietic responses to

doses that increased RBC, the coefficients of the model indicate that despite having a lower potency, CNTO 530 caused a more rapid mobilization of RET. The results of the PK/PD modeling suggest that CNTO 530 stimulates erythropoiesis in a similar fashion to epoetin-α and darbepoetin-α and that the PK properties of an ESA are the most important factor in determining efficacy. In addition, dose threshold is an important factor we need to consider in designing the PK/PD model. Understanding dose threshold of a drug aids in determining appropriate dose levels and, therefore, helps diminish side effects of the compound and reduces treatment costs. Many studies have focused on non-quantitative analysis of drug dose threshold, which can be biased by various factors. Aiming for quantitative analysis of this parameter, we proposed two statistical methods to determine dose threshold of a drug and applied them to CNTO 530.

Chapter 1: Biological Background

1.1 Physiology of Erythropoiesis

Erythropoiesis is a complicated process by which red blood cells are produced from bone marrow and then mature in the circulation. In this process, a hematopoietic stem cell (HSC) undergoes a series of differentiations (Koury et al., 2002). As seen in Figure 1.1, inside the bone marrow, a HSC firstly grows to a burst forming unit-erythroid (BFU-E). Then the BFU-E undergoes some changes to become a colony forming unit-erythroid (CFU-E). This CFU-E becomes morphologically identifiable erythroid precursor with cytoplasm: proerythroblast (Pro-EB), basophilic-erythroblast (Baso-EB), polychromatophilic-erythroblast (Poly-EB) and orthochromic-erythroblast (Ortho-EB). Later, the cell develops into an immature red blood cell called a reticulocyte (RET) in the bone marrow and is then released into the blood stream. Ultimately it becomes a mature red blood cell (RBC_M). After the Poly-EB stage, erythroid cells undergo highly specialized maturation, and their nuclei shrink with condensed chromatin. RBC_M are biconcave disks with no nucleus and are composed mostly of hemoglobin.

There are several factors regulating erythropoiesis. A major regulator of erythropoiesis in mammals is erythropoietin (EPO) (Krantz, 1991). EPO is a glycoprotein hormone produced mainly by the peritubular cells in the kidneys (Wu et al., 1995). It binds to the erythropoietin receptor (EPO-R) on the cell surface and activates several

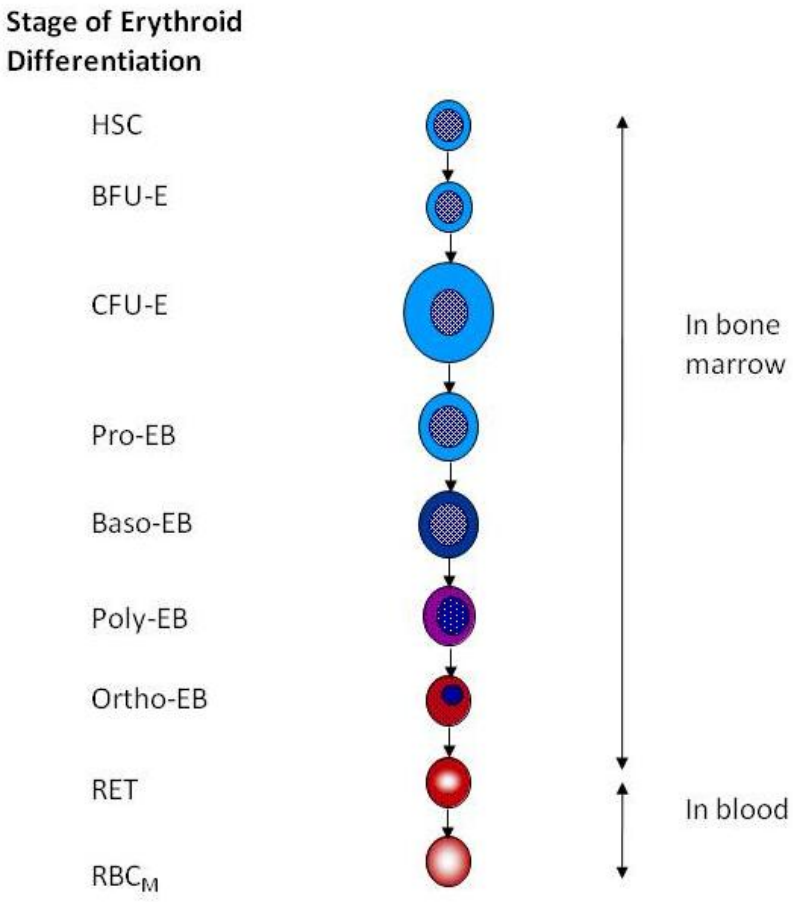

Figure 1.1: The relative sizes and nucleus to cytoplasm ratios of erythroid cells at various stages of erythropoiesis (adapted from (Bugelski, 2005; Koury et al., 2002): the color of the cytoplasm describing the relative content of ribosomes (dark blue) and hemoglobin (red).

signal transduction pathways (Fisher, 2003; Richmond et al., 2005). CFU-E has the highest number of EPO-R and therefore is the primary target cell in the bone marrow acted on by EPO (Fisher, 1997). Binding with EPO-R, EPO not only increases the number of erythroid precursors but also accelerates the release of reticulocytes from the bone marrow without markedly altering the cell cycle length or number of mitotic divisions involved in the differentiation process (Spivak, 1986). Additionally, EPO may decrease the rate at which EPO-dependent progenitor cells undergo pro-

grammed cell death (apoptosis) (Fisher, 1997). Blood oxygenation can also affect the erythropoiesis process (Koury et al., 2002). It is a feed-back mechanism: oxygen tension in blood regulates erythropoiesis process and hemoglobin is responsible for oxygen delivery, changing oxygen level.

1.2 Erythropoiesis Stimulating Agents

The malfunction or lack of EPO can severely disrupt the production of red blood cells, which can potentially lead to anemia. Erythropoiesis Stimulating Agents (ESAs) are agents, structurally and biologically, similar to endogenous EPO and were developed to help treat anemia. In our research, we studied three ESAs: epoetin-α, darbepoetin-α, and CNTO 530. Epoetin-α and darbepoetin-α have been widely used with patients whose normal erythropoietic processes have been undermined due to chronic renal failure, certain types of cancer or AIDS (Bunn, 2007; Jelkmann, 2002). CNTO 530 is a novel erythropoiesis stimulating agonist newly developed by Centocor Ortho Biotech Products, L.P..

1.2.1 Two commercially available ESAs

Epoetin-α, sometimes referred to as recombinant human erythropoietin (rHuEPO), is an exogenous EPO manufactured by recombinant DNA technology. It contains the identical amino acid sequence and has the same biological effects as endogenous EPO (Egrie et al., 1986). It is marketed by Centocor Ortho Biotech Products, L.P. under the trade name Procrit® and by Amgen Inc. under the trade name Epogen®. Both of them are man-made injectable drugs for treating anemia.

Darbepoetin-α is a hyperglycosylated epoetin-α analogue, containing five N-linked carbohydrate chains, two more than epoetin-α (Egrie and Browne, 2001). In the study conducted by Egrie and Browne (2001), sialic acid-containing carbohydrates of EPO are directly related to its circulating half-life, and *in vivo* biological activity, but inversely related to its receptor-binding affinity. Due to its additional carbohydrate chains, darbepoetin-α has approximately a 4-fold lower EPO-R binding activity, a 3-fold longer circulating half-life and greater *in vivo* biological activity than epoetin-α (Egrie et al., 2003). It is marketed by Amgen Inc. under the trade name Aranesp®. Similar to epoetin-α, darbepoetin-α is produced using recombinant DNA technology.

1.2.2 One newly developed ESA

CNTO 530 is a newly designed ESA which is different from epoetin-α and darbepoetin-α since it has no sequence homology with EPO. It is an antibody Fc domain fusion protein containing two erythropoietin mimetic peptide-1 (EMP1) sequences as a pharmacophore (Bugelski et al., 2008). It mediates different physiological effects by binding to various cell receptors. EMP1 is a non-erythropoietin derived EPO-R agonist. It binds to EPO-R and mediates the same signal transduction systems to produce similar effects as EPO. Fusion proteins are molecular constructs in which two genes are joined together and express as a single gene product. Since CNTO 530 is an antibody fusion protein where two EMP1 sequences are linked to the Fc domain, it can bind to EPO-R and express EPO-liked bioactivity while the Fc domain provides for extended pharmacokinetic properties.

1.2.3 Different biological properties

ESAs can have very different chemical and biological properties as has been shown in previous studies (Bugelski et al., 2007; Bunn, 2007; Egrie et al., 2003). Epoetin-α has a relatively short terminal half-life of 4-8 hours in humans and needs to be administrated 2-3 times a week (Faulds and Sorkin, 1989; Jelkmann, 2002). In addition, some patients have developed anti-EPO antibodies due to immunogenicity which can reduce the benefit of taking epoetin-α (Bunn, 2007). Compared with epoetin-α, darbepoetin-α has a longer half-life of 25.3 to 48.8 hours in humans (Macdougall, 2001), and greater *in vivo* biological activity, which allows for less frequent administration (Bunn, 2007). Although it has not been tested in humans, CNTO 530 has shown a terminal half-life of 40 hours in mice (Bugelski et al., 2008; Sathyanarayana et al., 2009) and 72 hours in rats after a single s.c. administration (Martin et al., 2010). In comparison, the half-lives for epoetin-α and darbepoetin-α in rats after a single s.c. administration are 7.8 hours (Woo et al., 2006) and 15 hours (Yoshioka et al., 2007), respectively.

Chapter 2: Background on Pharmacokinetic and Pharmacodynamic Analysis

Pharmacokinetics explores what the body does to the drug, i.e., the movement of a drug into, through, and out of the body. Pharmacodynamics explores what a drug does to the body, i.e., the physiological effects of drugs on the body and the mechanisms of drug action. Pharmacodynamics (PD) combined with pharmacokinetics (PK) helps explain the relationship between the drug dose and response (see Figure 2.1). Both are very complex biological processes and mathematical models have been developed to explore the biological mechanisms of drugs.

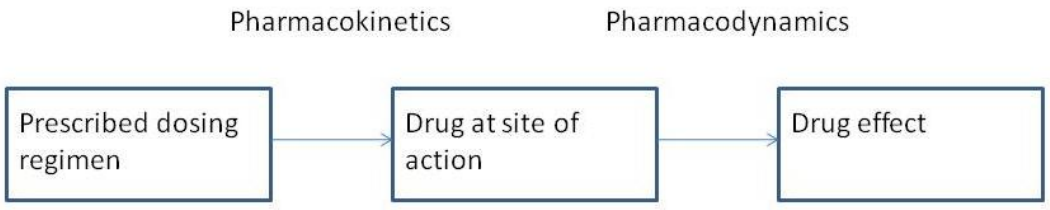

Figure 2.1: Relationship between pharmacokinetics and pharmacodynamics.

Combined PK/PD studies focus on these two important subjects of pharmacology and build connections between them (Derendorf and Meibohm, 1999). They link the time course of drug concentration as assessed by pharmacokinetics to the time-invariant relationship between the concentration at the application site and the effect intensity as characterized by pharmacodynamics (see Figure 2.2). Thus, PK/PD models allow us to describe the time course of the effect intensity resulting from the

administration of a certain dosage regimen. Levy (1964) did the pioneering work to link the pharmacokinetics of a drug with the subsequent *in vivo* pharmacological response. Widespread use of PK/PD concepts started in early 1980 when the temporal dissociation between the effect intensity and the drug concentration could be solved by the effect-compartment model developed by Sheiner and coworkers (Holford and Sheiner, 1981a,b, 1982; Sheiner et al., 1979).

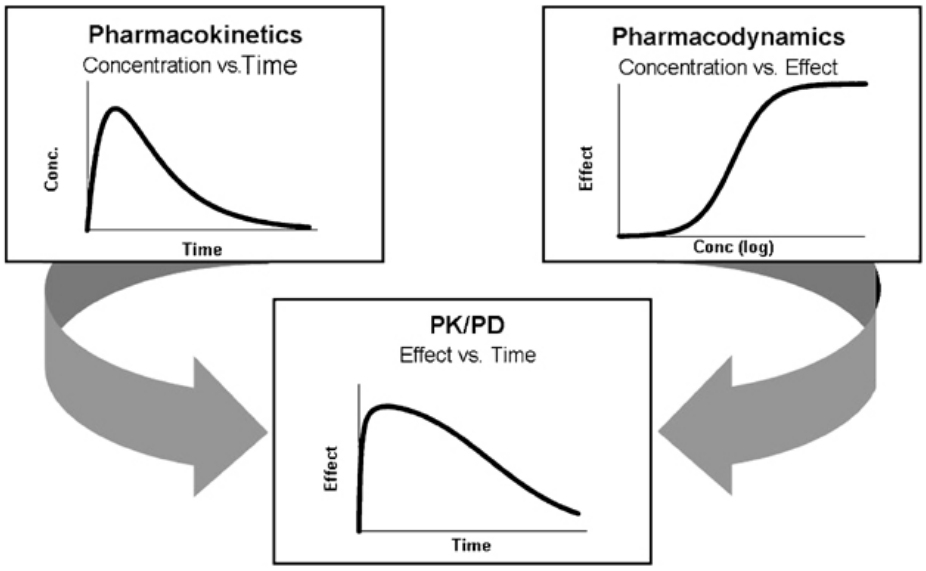

Figure 2.2: PK/PD modeling as combination of two pharmacological processes: pharmacokinetics describing concentration-time courses of drugs and pharmacodynamics describing effect-concentration relationships of drugs. Source: (Derendorf and Meibohm, 1999)

This thesis studied biological properties of three ESAs, epoetin-α, darbepoetin-α and CNTO 530. It is important to compare pharmacokinetics and pharmacodynamics to determine differences between biological properties of these ESAs. The differences may help doctors better choose the most appropriate treatment option for anemic patients. However, in practice it can be difficult to make a meaningful comparison between two sets of parameters obtained from two different PK/PD models.

It is known that epoetin-α, darbepoetin-α, and CNTO 530 have similar molecular mechanisms which initiate several signal transduction pathways by binding EPO-R to stimulate red blood cell production (Bugelski et al., 2008; Egrie and Browne, 2001; Egrie et al., 1986). Due to these similarities it may be possible to use a single PK/PD model structure to describe these three ESAs. If such a model can be found, a direct mathematical comparison of PK/PD parameters can be made across all three ESAs. However, few attempts have been made to develop a single PK/PD model for multiple ESAs.

2.1 Pharmacokinetic Analysis

Generally, as shown in Figure 2.3, there are four processes studied by pharmacokinetics (Gibaldi and Perrier, 1982; Groulx, 2006):

- Absorption is the process by which a drug infiltrates from an administration site into the bloodstream of the body. A drug can be administered through various routes, such as intramuscular (i.m.), intravenous (i.v.), subcutaneous (s.c.), oral, etc.

- Distribution is the process by which a drug is transported through body fluids from the bloodstream to the tissues of the body. It is assumed that the drug is uniformly distributed throughout the body.

- Metabolism is the process by which a drug is chemically inactivated in preparation for elimination from the body. Some drugs are metabolized quickly, while others can take longer before they are eliminated.

- Excretion is the process by which a drug is eliminated from the body. Immediately after administration of a drug , the body begins to eliminate via hepatic metabolism, renal excretion, or both.

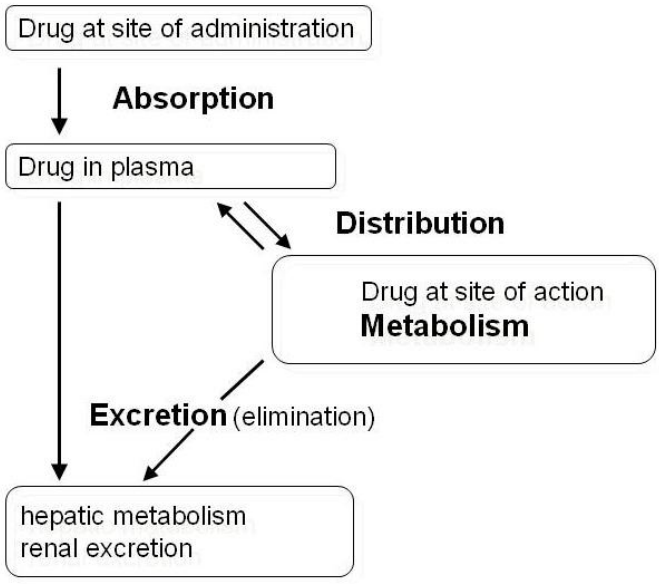

Figure 2.3: Four processes involved in pharmacokinetics: absorption, distribution, metabolism and excretion (ADME).

In order to provide safe and effective dose to patients, it is essential to understand how a drug interacts with the body at different dose level. However, unless a drug has the property of dose proportionality, obtaining a complete pharmacokinetic profile for all possible doses of a drug is difficult. Dose proportionality implies that the rates of absorption, distribution, metabolism, and elimination remain constant over a certain dose range (Gibaldi and Perrier, 1982). Many drugs have the property in their therapeutical range, which makes it easier to study their PK effects (Gabrielsson and Weiner, 2007).

Pharmacokinetic analysis can be conducted by either non-compartmental analysis or compartmental analysis (Gibaldi and Perrier, 1982). Non-compartmental analysis uses numeric methods to estimate the exposure to a drug (Yoshioka et al., 2007). The advantage of non-compartmental analysis is that it requires fewer assumptions than those which are necessary with compartmental analysis. The disadvantage of non-compartmental analysis is that it highly depends on the blood/plasma sampling schedule. Compartmental analysis uses kinetic models to describe and predict the concentration-time curve. The advantage of compartmental analysis is its ability to predict the concentration at any time. In addition, with the property of dose proportionality, PK compartmental models of a drug could help predict the concentration versus time profiles at other dose levels. The disadvantage of compartmental analysis is the difficulty in developing and validating such models.

2.1.1 Non-compartmental pharmacokinetic analysis

Many studies have used non-compartmental pharmacokinetic analysis (Bugelski et al., 2008; Cheung et al., 1998; Yoshioka et al., 2007). There are eight important non-compartmental model parameters:

- AUC: the area under the concentration-time curve. This term can be used to calculate overall clearance values for a drug. In addition, AUC is frequently used to compare drug exposures achieved with different drug doses.

- V_d: volume of distribution. It is the theoretical volume of fluid into which the total amount of drug administered would have to be uniformly distributed to produce the drug concentration in plasma. It is an important indicator of the

extent of drug distribution into fluids and tissues. Initial drug concentration is calculated as drug dose divided by V_d. A large volume of distribution indicates that the drug distributes extensively into body tissues and fluids. Conversely, a small volume of distribution indicates limited drug distribution (DiPiro et al., 2005).

- F: Bioavailability, the fraction of drug that is absorbed. It is used to describe how much drug reaches the circulation system after administration. The bioavailability of an i.v. drug dose is assumed to be 100%. In the case of s.c. and oral administration, F is calculated as the ratio of drug concentration after giving the drug, compared with the same dose given intravenously.

- $t_{1/2}$: terminal half-life. It is defined as the time required for the concentration of a drug to decrease by 50% of the current concentration in the final elimination phase. If a drug follows first-order elimination, then it would take about 5-6 half-lives for the drug to be completely removed from the body.

- λ_z: terminal elimination rate constant. It is defined as the exponential rate at which drugs are removed from the body in the final elimination phase. There is a relationship between λ_z and $t_{1/2}$:

$$\begin{aligned} t_{1/2} &= \frac{\ln(C_{drug}) - \ln(0.5C_{drug})}{\lambda_z} \\ &= \frac{\ln 2}{\lambda_z} \end{aligned}$$

where C_{drug} is the drug concentration in the plasma or serum.

- CL: the volume of plasma from which the drug is completed removed per unit time. CL/F, apparent clearance, is used in the cases of s.c. and oral administration. CL or CL/F can be calculated using formula $Dose/AUC$.

- C_{max} and T_{max}: after a drug is administered at time 0, its concentration will reach a peak level, C_{max}, at time T_{max}.

2.1.2 Compartmental pharmacokinetic analysis

Compartmental models are categorized by the number of compartments required to describe the drug's behavior in the body. There are one-compartment, two-compartment, and multi-compartment models. They can be mathematically expressed using linear differential equations or non-linear differential equations (Sheiner, 1984, 1985, 1986). The compartments do not necessarily represent a specific tissue or fluid but may represent a group of similar tissues or fluids. Because of dose proportionality, these models can be used to predict concentration versus time profiles of a drug in the body in the therapeutical range.

For one-compartmental models (Dayneka et al., 1993; Krzyzanski and Jusko, 1998), the body is assumed to be a single compartment. As shown in Figures 2.4 and 2.5, the model structure for i.v. dosing is slightly different from the one for s.c. dosing. For both of them, $C(t)$ is the concentration of drug in the plasma at time t, and K_{el} is a first order elimination rate. For s.c. dosing, the model structure has two additional items: $Input(t)$ is the concentration of drug at the s.c. injection site at time t and K_a is a first order absorption rate.

The following differential equation describes the one-compartmental PK model for

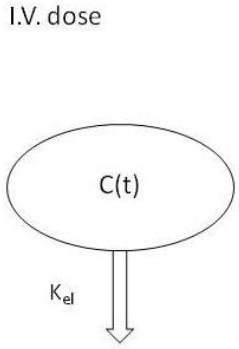

Figure 2.4: A general one-compartmental PK model for i.v. dosing.

i.v. dose in Figure 2.4:

$$\frac{dC(t)}{dt} = -K_{el} \times C(t)$$

Initially, $C(0) = Dose/V_d$. There are two model parameters: K_{el} and V_d (volume of distribution).

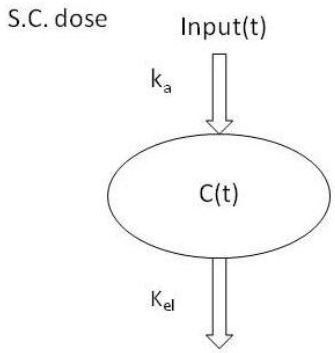

Figure 2.5: A general one-compartmental PK model for s.c. dosing.

The following differential equations describe the one-compartmental PK model for

s.c. dose in Figure 2.5:

$$\begin{aligned} \frac{dC(t)}{dt} &= K_a \times Input(t) - K_{el} \times C(t) \\ \frac{dInput(t)}{dt} &= -K_a \times Input(t) \end{aligned}$$

Initially, $C(0) = 0$ and $Input(0) = Dose \times F/V_d$. There are three model parameters: K_{el}, V_d, and K_a.

For basic two-compartment models (Agoram et al., 2006; McLennan et al., 2006), the central compartment includes the blood and well perfused organs, such as the heart, lungs, liver and kidneys. The peripheral compartment includes poorly perfused tissues and organs, such as the fat tissue, muscle tissue, and cerebrospinal fluid. Similar to one-compartmental PK models, the two-compartmental PK model for s.c. dosing has one more variable ($Input(t)$) and one more rate (K_a) than the one for i.v. dosing (see Figure 2.6 and 2.7)

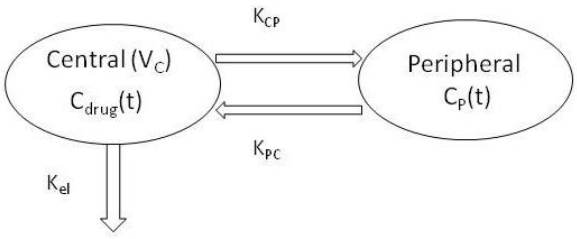

Figure 2.6: A general two-compartmental PK model for i.v. dosing.

The following differential equations describe the two-compartmentl PK model for

i.v. dose in Figure 2.6:

$$\begin{aligned} \frac{dC_{drug}(t)}{dt} &= -(K_{el} + K_{CP}) \times C_{drug}(t) + K_{PC} \times C_P(t) \\ \frac{dC_P(t)}{dt} &= K_{CP} \times C_{drug}(t) - K_{PC} \times C_P(t) \end{aligned}$$

where $C_{drug}(t)$ and $C_P(t)$ are the concentration of drug in the central (blood and well perfused organs) and peripheral (poorly perfused tissues) compartments at time t, K_{CP} and K_{PC} are two inter-compartment exchange rates, and V_C is the volume of distribution in the central compartment. Initially, $C_{drug}(0) = Dose/V_C$ and $C_P = 0$. There are four model parameters: K_{el}, V_C, K_{CP}, and K_{PC}.

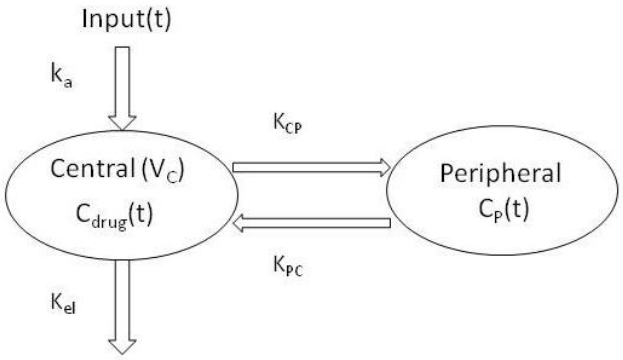

Figure 2.7: A general two-compartmental PK model for s.c. dosing.

The following differential equations describe the two-compartmental PK model for s.c. dosing in Figure 2.7:

$$\begin{aligned} \frac{dC_{drug}(t)}{dt} &= K_a \times Input(t) - (K_{el} + K_{CP}) \times C_{drug}(t) + K_{PC} \times C_P(t) \\ \frac{dC_P(t)}{dt} &= K_{CP} \times C_{drug}(t) - K_{PC} \times C_P(t) \\ \frac{dInput(t)}{dt} &= -K_a \times Input(t) \end{aligned}$$

Initially, $C_{drug}(0) = 0$, $C_P(0) = 0$ and $Input(0) = Dose \times F/V_C$. There are five model parameters: K_{el}, V_C, K_{CP}, K_{PC}, and K_a.

Basic compartmental models can be changed to non-linear models by introducing complicated absorption or excretion processes. For example, a complicated absorption process may consist of dual absorption rates which combine a zero-order rate and a first-order rate (Cheung et al., 2004; Ramakrishnan et al., 2003; Woo et al., 2006). A complicated excretion process may involve Michaelis-Menten elimination (Cheung et al., 2004) only, or both a first-order elimination and a Michaelis-Menten elimination (Kato et al., 1997, 2001).

We used a one-compartment PK model to explain Michaelis-Menten elimination (see Figure 2.8).

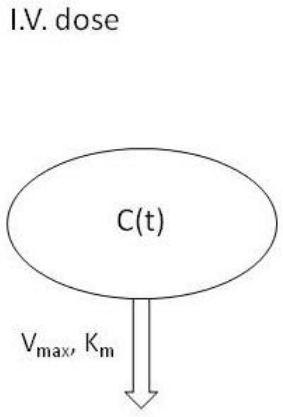

Figure 2.8: A one-compartmental PK model for i.v. dosing with Michaelis-Menten elimination.

The following differential equation describes the nonlinear PK model in Figure

2.8:

$$\frac{dC(t)}{dt} = -\frac{V_{max} \times C(t)}{K_m + C(t)}$$

where V_{max} is the maximum elimination rate, and K_m is the plasma drug concentration at which the elimination rate reaches 50% V_{max}. The rate of drug elimination ($V_{max} \times C(t)/(K_m + C(t))$) changes as a function of drug concentration as demonstrated in Figure 2.9. At high concentrations ($C(t) >> K_m$), the plasma drug concentrations decline at zero-order rate equal to V_{max}. At very low concentrations ($C(t) << K_m$), the plasma drug concentrations decline at first-order rate V_{max}/K_m. At intermediate concentrations, the plasma drug concentrations decline at a variable rate as function of the varying plasma drug concentrations themselves.

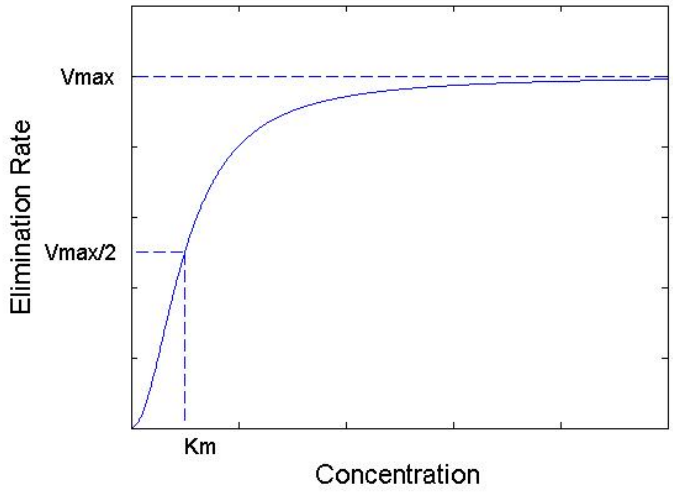

Figure 2.9: The saturation curve of Michaelis-Menten elimination.

Most drugs in the therapeutic range are at the bottom of the Michaelis-Menten curve and obey linear pharmacokinetics and making their this is why their plasma concentration versus time curves exponential (Mehvar, 2001).

2.2 Pharmacodynamic Analysis

The field of pharmacodynamic modeling has gained many advances recently because of the development of basic and extended mechanism-based models (Mager et al., 2003). We will focus on four classes of PD modeling approaches to illustrate their challenges and complexities, but also opportunities to characterize the pharmacodynamics of drugs (Crommelin et al., 2008; Derendorf and Meibohm, 1999).

- Direct response PD models;
- Indirect response PD models;
- Cell lifespan PD models;
- *Ad-hoc* response PD models.

2.2.1 Direct response PD models

For the direct response PD models, it is assumed that the observed effect is determined by the effect site concentrations without time lag. In this case, maximum effects are assumed to occur simultaneously with maximum effect site concentrations of the drug. (Derendorf and Meibohm, 1999).

The classical direct response PD model is the sigmoid E_{max} model (Mager et al., 2003) as demonstrated in Figure 2.10:

$$Ef(t) = \frac{E_{max} \times C(t)^n}{EC_{50}^n + C(t)^n}$$

where $Ef(t)$ is the variable of pharmacological effect, E_{max} is the maximum achievable

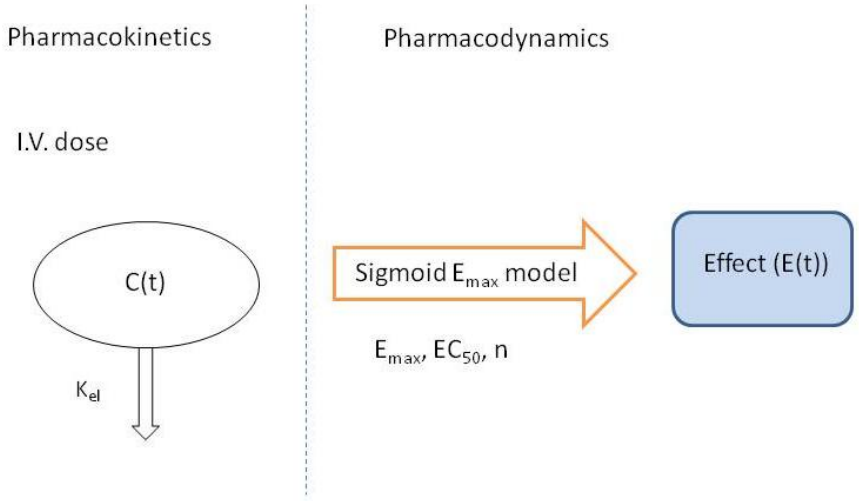

Figure 2.10: Diagram of a typical direct response PD model. It is also a sigmoid E_{max} model (adapted from (Crommelin et al., 2008)).

effect, EC_{50} is the drug concentration that produces half of the maximum effect and n is the shape factor that allows for an improved fit of the relationship to the observed data. In other words, E_{max} represents the efficacy of the drug in the system. EC_{50} helps characterize the potency of the drug in the system, i.e., the sensitivity of the organ or tissue to the drug (Derendorf and Meibohm, 1999).

2.2.2 Indirect response PD models

There often is temporal dissociation between the time course of drug concentration and the drug effect (Dayneka et al., 1993). Such concentration-effect relationships of many drugs could be characterized by an indirect response model. In this model, maximum plasma concentrations will occur before maximum effects of the drug (Crommelin et al., 2008). Moreover, the effect intensity will increase despite decreasing plasma concentrations and may continue beyond the time when drug concentrations

in plasma are no longer detectable.

Early in 1993, Dayneka et al. (1993) proposed four basic models for characterizing indirect PD responses after drug administration which have been widely used in studying the pharmacodynamics of numerous drugs. In each variant, the synthesis or degradation process of the response is either stimulated or inhibited as a function of the drug concentration at the effect site. Schematics of the four basic indirect response models are shown in Figure 2.11. Their corresponding differential equations are given as follows:

$$\begin{aligned}
\text{(a)} \quad \frac{dR(t)}{dt} &= k_{in} \times II(t) - k_{out} \times R(t) \\
\text{(b)} \quad \frac{dR(t)}{dt} &= k_{in} - k_{out} \times II(t) \times R(t) \\
\text{(c)} \quad \frac{dR(t)}{dt} &= k_{in} \times SS(t) - k_{out} \times R(t) \\
\text{(d)} \quad \frac{dR(t)}{dt} &= k_{in} - k_{out} \times SS(t) \times R(t)
\end{aligned}$$

where $R(t)$ is the variable for response to a drug, K_{in} is the zero-order constant for production of the response and K_{out} is the first-order rate constant for loss of the response.

Inhibitory function $II(t)$ and stimulatory function $SS(t)$ are modeled using sigmoid model:

$$\begin{aligned}
II(t) &= 1 - \frac{C(t)}{IIC_{50} + C(t)} \\
SS(t) &= 1 + \frac{SS_{max} \times C(t)}{SSC_{50} + C(t)}
\end{aligned}$$

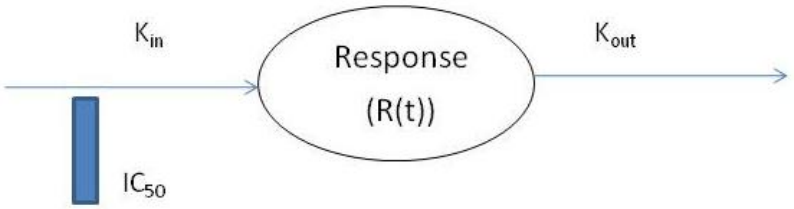

(a)

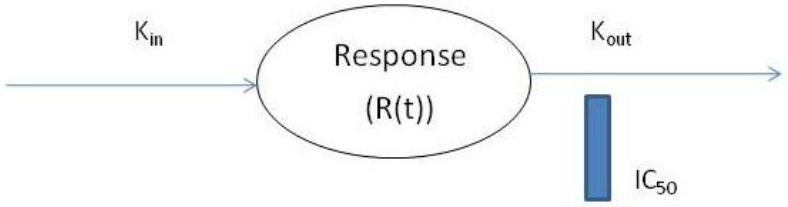

(b)

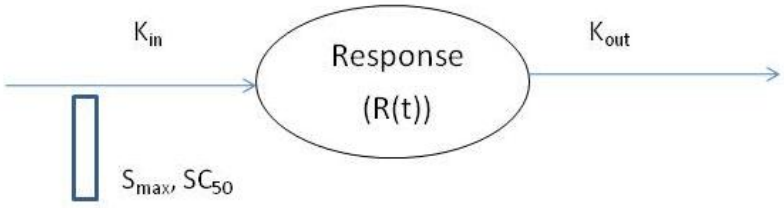

(c)

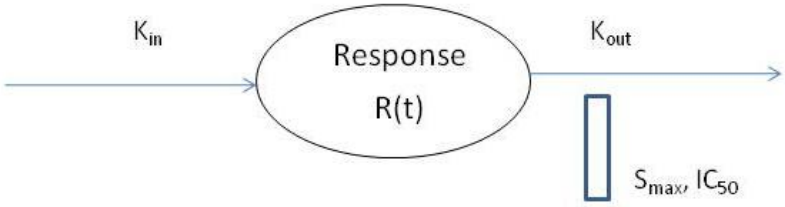

(d)

Figure 2.11: Schematics of four basic indirect response PD models (Dayneka et al., 1993) characterized by either inhibition or stimulation of the response variable.

where $C(t)$ represents plasma concentration of a drug as a function of time, IIC_{50} is the drug concentration which produces half of maximum inhibitory effect, SS_{max} represents maximum stimulation of responses by a drug and SSC_{50} represents the drug concentration for producing 50% maximum stimulation of response.

More reviews and assessments of these four basic indirect response models were conducted by (Krzyzanski and Jusko, 1998; Sharma and Jusko, 1996). They provided useful information as to appropriate model selection, model sensitivity to parameter values and dose levels, and methods of obtaining initial parameter estimates from experimental data. Furthermore, Yao et al. (2006) included empirical lower and upper limits in the basic indirect response models to characterize drug response for turnover systems which are maintained within a certain range.

2.2.3 Cell life span PD models

Similar to indirect response models, cell life span models are also developed based on underlying cellular processes. They model the mechanisms of the sequential maturation and lifespan-driven cell turnover of drug affected cell types and progenitor cell populations (Crommelin et al., 2008). In particular, there are a number of protein compounds taking effect through direct or indirect regulation of blood and/or immune cells. For these kinds of protein compounds, cell life span models have been proven useful to describe and predict their effects (Krzyzanski et al., 1999; Perez-Ruixo et al., 2005). They are widely used for characterizing the dose-concentration-effect relationships of hematopoietic growth factors which modify erythropoiesis, granulopoiesis, or thrombopoiesis (Krzyzanski et al., 1999; Perez-Ruixo et al., 2005). These pro-

cesses consist of sequential maturation of a series of cell types. The delay between drug administration and the observed response of hematopoietic growth factors is mainly accounted for by the fixed physiological time span for the maturation of precursor cells, i.e., change in the cell count in peripheral blood. Cell life span models accommodate this sequential maturation of multiple types of cells by a series of transit compartments linked via first- or zero-order processes with a common constant transfer rate.

A typical cell life span PD model is shown in Figure 2.12. This model can be described using the following differential equation:

$$\frac{dR(t)}{dt} = k_{in} \times SS(t) - k_{in} \times SS(t - T_R) \tag{2.1}$$

where, T_R is the average cell life-span.

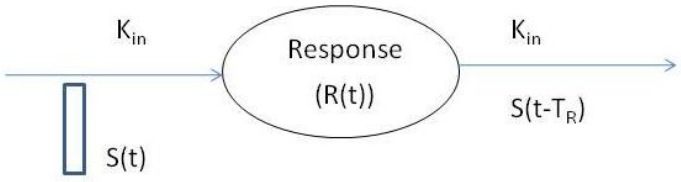

Figure 2.12: Schematic of a typical cell lifespan model (Krzyzanski et al., 1999).

2.2.4 *Ad-hoc* response PD models

Since the effect of many protein compounds is mediated via complex regulatory physiologic processes including feedback mechanisms and/or tolerance phenomena, some PD models have been developed to account for unique physiologic processes of some protein drugs. On one hand, *ad-hoc* models may better describe individual drugs,

and catch more details and thus are often much more sophisticated than the three models previously discussed. On the other hand, they are not applicable as widely as previous models due to lack of common ground.

2.3 Original Contributions

To facilitate the comparison of PK/PD model parameters for epoetin-α, darbepoetin-α and CNTO 530, we developed a single PK/PD model for the three drugs. We used a standard PK model (DiPiro et al., 2005) to predict the concentration profiles of the dugs. We developed a new indirect response PD model which incorporated the combined effect of stimulation from the drug and inhibition from hemoglobin on the conversion of RETs to mature RBCs. The PK/PD model was then tested using experimental data for rats and it was found that our PK/PD model fits data collected from all three drugs over a period of at least 72 days (1728 hours), which is longer than previous experiments. We also discovered that the PD parameters for CNTO 530 are different from those of epoetin-α and darbepoetin-α. This suggests that the hematological response of CNTO 530 is different from those of epoetin-α and darbepoetin-α that does not only depend on their pharmacokinetics.

Furthermore, we developed a new statistical criterion which used our model to predict dose threshold of a drug. In addition, we designed a normal range criterion which can be used when control data are available. The methods were successfully applied to the CNTO 530 data set.

Chapter 3: Our Pharmacokinetic/Pharmacodynamic Model

Pharmacokinetic models of erythropoiesis stimulating agents have been extensively studied in the literature (Agoram et al., 2006; Ette and Williams, 2007; Khorasheh et al., 1999). After testing various model structures we found that a simple linear two-compartmental PK model may be applicable on three ESAs that we studied. However, existing PD models do not fit our data for up to 72 days. For example, we found that existing indirect response models lacked a negative feedback and cell lifespan models were not robust enough for analyzing drug response up to 72 days. So we developed a new indirect response PD model that includes negative feedbacks and is suitable for longer response periods.

3.1 Pharmacokinetic Model

Figure 3.1 shows the linear two-compartment PK model containing an absorption rate K_a, two inter-compartment exchange rates (K_{CP} and K_{PC}) and an elimination rate K_{el} that we chose for our data (DiPiro et al., 2005).

The following differential equations describe this model:

$$\frac{dC_{drug}(t)}{dt} = K_a \times Input(t) - (K_{el} + K_{CP}) \times C_{drug}(t) + K_{PC} \times C_P(t) \quad (3.1)$$

$$\frac{dC_P(t)}{dt} = K_{CP} \times C_{drug}(t) - K_{PC} \times C_P(t) \quad (3.2)$$

$$\frac{dInput(t)}{dt} = -K_a \times Input(t) \quad (3.3)$$

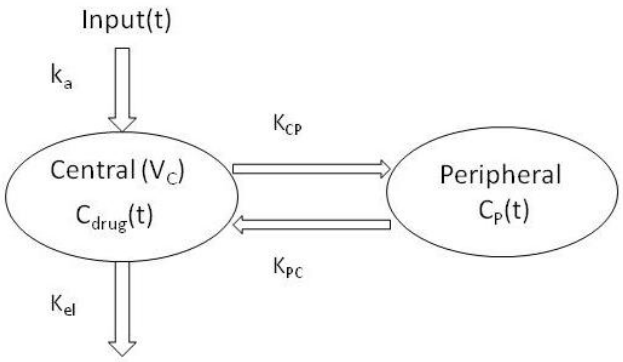

Figure 3.1: A two-compartmental PK model

where $C_{drug}(t)$ and $C_P(t)$ are the concentration of drug in the central (blood and well perfused organs) and peripheral (poorly perfused tissues) compartments at time t, and $Input(t)$ is the concentration of drug at the s.c. injection site at time t. Initial conditions are $C_{drug}(0) = 0$, $C_P(0) = 0$, and $Input(0) = (Dose \times F)/V_C$, where F represents the bioavailability of the subcutaneously administrated drug and V_C is the volume of distribution in the central compartment.

Eq. 3.1–3.3 are linear differential equations, where the analytical solution of $C_{drug}(t)$ can be expressed as:

$$C_{drug}(t) = \frac{Dose}{F}(Ae^{-\alpha t} + Be^{-\beta t} - (A+B)e^{-K_a t}) \tag{3.4}$$

where

$$\alpha = \left((K_{el} + K_{CP} + K_{PC}) + \sqrt{(K_{el} + K_{CP} + K_{PC})^2 - 4(K_{el}K_{PC})}\right)/2 \tag{3.5}$$

$$\beta = \left((K_{el} + K_{CP} + K_{PC}) - \sqrt{(K_{el} + K_{CP} + K_{PC})^2 - 4(K_{el}K_{PC})}\right)/2 \tag{3.6}$$

$$A = \frac{(K_{PC} - \alpha)K_a}{V_C(K_a - \alpha)(\beta - \alpha)} \tag{3.7}$$

$$B = \frac{(K_{PC} - \beta)K_a}{V_C(K_a - \beta)(\alpha - \beta)} \tag{3.8}$$

$$\tag{3.9}$$

3.2 Pharmacodynamic Model

We developed an indirect response PD model with feedback regulatory loops (Figure 3.2) to characterize the erythropoietic effects of drugs. Based on the progression of erythropoiesis as shown in Figure 3.3. There are four compartments in our model: (1) Early Stages, representing erythroid progenitors and erythroblasts, (2) RET, reticulocyte, (3) $\mathrm{RBC_M}$, mature red blood cell, and (4) HGB, hemoglobin level. Unlike previous studies (Agoram et al., 2006; Krzyzanski et al., 2005; Woo et al., 2006), our model does not incorporate changes in the compartment of early stages or bone marrow. Instead, a variable $K_{in}(t)$ is used to model the production rate or release of reticulocyte cells into the bloodstream. The change in $K_{in}(t)$ over time is controlled by an inflow rate which is proportional to drug stimulation effect $S(t - T_d)$ and hemoglobin inhibition effect $I(t - T_d)$ and an outflow rate which is proportional to itself (Eq. 3.10). T_d is the time to mobilize reticulocytes and RBC after administration of a ESA. In the model, K_{out1} and K_{out2} are defined as elimination rates of RET and $\mathrm{RBC_M}$ states respectively. We assume that there is a combined effect from drug concentration ($E_1(t)$) and change of hemoglobin level ($E_2(t)$), which affect how reticulocytes become mature RBCs. We define $E(t) = E_1(t) + E_2(t)$ to model this effect, so that at equilibrium, $E(t)$ equals 1, $E(t)$ is smaller than 1 if inhibition

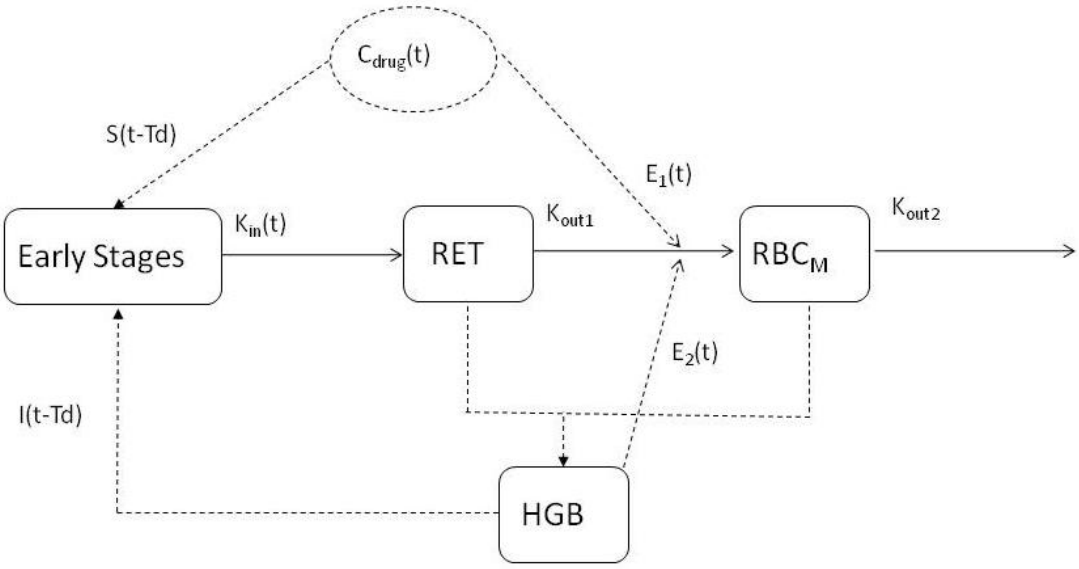

Figure 3.2: A diagram showing our PD model.

dominates, and larger than 1 if stimulation dominates.

The differential equations for the two compartments are as follows:

$$\frac{dK_{in}(t)}{dt} = K_p \times S(t - T_d) \times I(t - T_d) - K_{in}(t) \times K_e \tag{3.10}$$

$$\frac{dRET(t)}{dt} = K_{in}(t) - RET(t) \times K_{out1} \tag{3.11}$$

$$\frac{dRBC_M(t)}{dt} = RET(t) \times K_{out1} \times E(t) - RBC_M(t) \times K_{out2} \tag{3.12}$$

where,

$$S(t) = 1 + \frac{S_{max} \times C_{drug}(t)}{SC_{50} + C_{drug}(t)} \tag{3.13}$$

$$I(t) = 1 - \frac{I_{max} \times \Delta HGB(t)}{IC_{50} + \Delta HGB(t)} \tag{3.14}$$

$$\Delta HGB(t) = HGB(t) - HGB_{baseline} \tag{3.15}$$

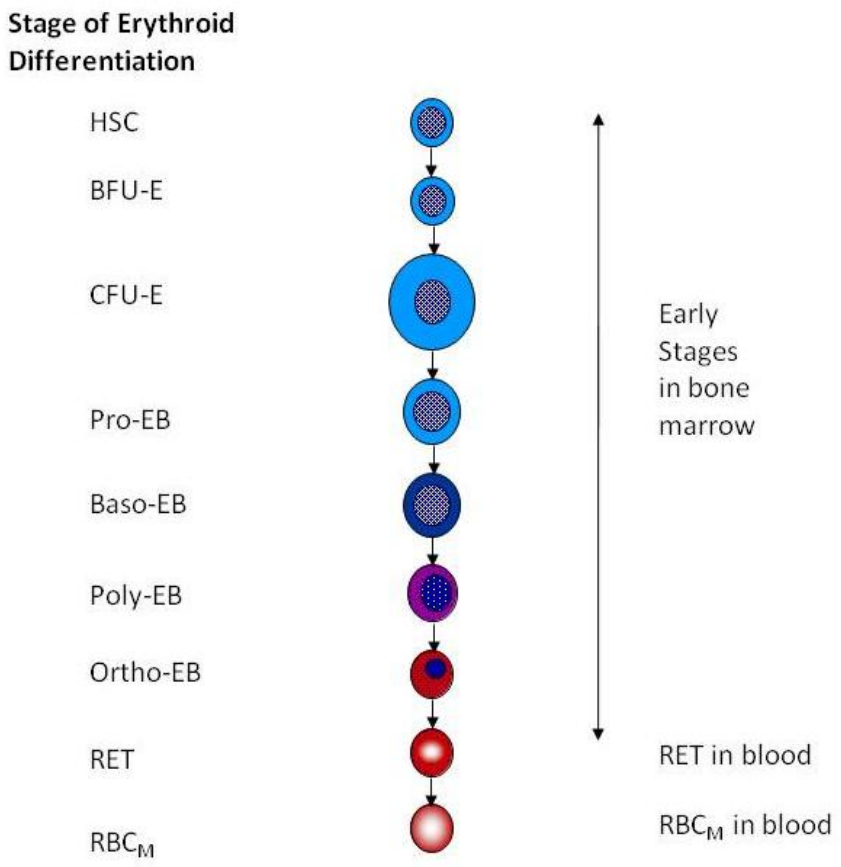

Figure 3.3: A diagram of erythropoiesis.

In the above equations, an indirect mechanism of drug action is assumed with the parameters, S_{max} which is the maximum stimulation of $K_{in}(t)$ and SC_{50} which is drug concentration required for producing 50% maximum stimulation of $K_{in}(t)$ (Dayneka et al., 1993). Because oxygen tension is a primary determinant of erythropoietic control and hemoglobin is responsible for oxygen delivery (Greer et al., 2003; Loeffler et al., 1989), a hemoglobin-driven feedback regulatory loop is used to characterize negative erythropoietic effects (Ramakrishnan et al., 2004; Woo et al., 2006). I_{max} is the maximum inhibition of $K_{in}(t)$ and is assumed to be equal to 1. IC_{50} is the hemoglobin change required for producing 50% maximum inhibition of $K_{in}(t)$.

Hemoglobin data were modeled with a simple linear model.

$$HGB(t) = RBC(t) \times MCH \tag{3.16}$$

where $RBC(t) = RET(t) + RBC_M(t)$ and MCH is mean corpuscular hemoglobin.

More information about the model parameters is needed to fit the model. Because the endogenous EPO level in the control group is very low (Woo et al., 2006), we assumed that the endogenous EPO is negligible and did not include it in the model. The initial conditions, $RET(0)$ and $RBC(0)$, were taken as baseline values calculated from the control group. $RBC_M(0)$ was calculated from $RBC(0)$ minus $RET(0)$. Without drug administration, $RET(t)$, $RBC(t)$ and $HGB(t)$ are assumed constant and E(t) equals 1. Therefore, the initial values of $K_{in}(0)$, K_P ($K_{in}(t)$ change rate), and K_{out2} ($\mathrm{RBC_M}$ eliminate rate) can be calculated using the following equations:

$$K_{in}(0) = RET(0) \times K_{out1} \tag{3.17}$$

$$K_P = K_{in}(0) \times K_e \tag{3.18}$$

$$K_{out2} = RET(0) \times K_{out1}/RBC_M(0) \tag{3.19}$$

Furthermore, we assumed that K_{out1} is determined by T_{RET} the mean lifespan of RET, i.e. $K_{out1} = 1/T_{RET}$.

3.3 Derivation of Effect Function $E(t)$

To complete our PD model, by defining E(t) we combined some compartments and simplified it as shown in Figure 3.4. Note that the sole purpose of this step is to help us solve Eq. 3.10–3.16. In this model, RET and $\mathrm{RBC_M}$ are combined into one compartment RBC. $K2_{out}$ is a constant first-order elimination rate of RBC. The variables $K2_{in}(t)$, $S2(t-T_d)$ and $I2(t-T_d)$ are analogous to the variables $K_{in}(t)$, $S(t-T_d)$ and $I(t-T_d)$ used in our model (Figure 3.2) and we assume that T_d is the same for both models.

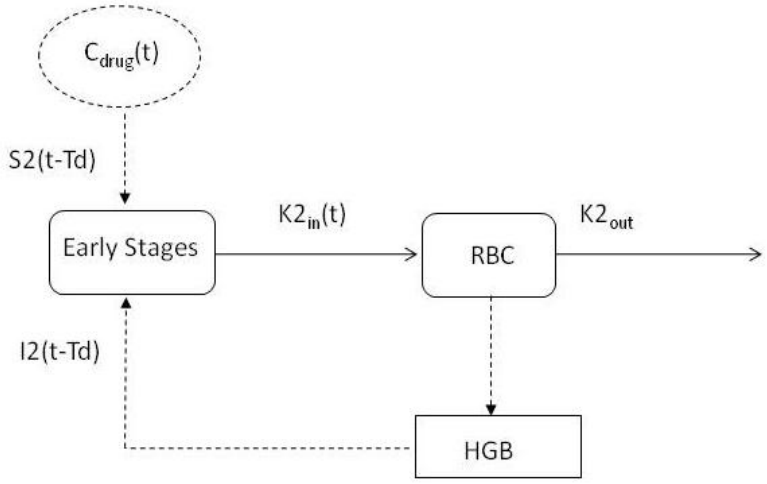

Figure 3.4: The simplified PD model applied to RBC counts for solving E(t).

From Figure 3.4, we derive the following differential equations:

$$\frac{dK2_{in}(t)}{dt} = K2_p \times S2(t-T_d) \times I2(t-T_d) - K2_{in}(t) \times K2_e \qquad (3.20)$$

$$\frac{dRBC(t)}{dt} = K2_{in}(t) - RBC(t) \times K2_{out} \qquad (3.21)$$

where,

$$S2(t) = 1 + \frac{S2_{max} \times C_{drug}(t)}{SC2_{50} + C_{drug}(t)} \tag{3.22}$$

$$I2(t) = 1 - \frac{\Delta HGB(t)}{IC2_{50} + \Delta HGB(t)} \tag{3.23}$$

The parameters $K2_P$, $K2_e$, $S2_{max}$, $SC2_{50}$, and $IC2_{50}$ are analogous to K_P, K_e, S_{max}, SC_{50}, and IC_{50} used in Eq. 3.10–3.16. Considering $K2_{out}(0) = K2_{in}(0)/RBC(0)$ (derived from Eq. 3.21 at time 0) and assuming $K2_{in}(0) = Kin(0)$, we are able to solve Eq. 3.10–3.12 along with Eq. 3.20–3.21. Finally, we could represent E(t) as follows:

$$E(t) = \frac{(K2_{in}(t) - K_{in}(t) + RBC_M(t) \times K_{out2} - RBC(t) \times K2_{out})}{RET(t) \times K_{out1}} + 1 \tag{3.24}$$

Chapter 4: Evaluation of PK/PD Model Using Biological Data

4.1 Agents

Epoetin-α was obtained from Ortho Biotech, Raritan, NJ. and darbepoetin-α (Aranesp, Amgen, Inc. Thousand Oaks, CA) was purchased commercially. CNTO 530 is an EPO-Mimetibody^{TM} construct that contains two EMP-1 sequences as the pharmacophore. EMP-1 is a 20-amino acid peptide that was discovered by screening combinatorial libraries of random sequence peptides using phage display technology (Johnson et al., 1998). EMP-1 binds to EPO-R and expresses EPO-like bioactivity in both *in vitro* and *in vivo* systems (Johnson et al., 1998; Livnah et al., 1998). EPO-Mimetibody^{TM} constructs were expressed in mammalian cells and purified by routine methods and supplied by Centocor R&D as described previously (Bugelski et al., 2008).

4.2 Rats

Female Sprague Dawley CD rats weighing approximately 300 grams were obtained from Charles Rivers Laboratories (Raleigh, NC). Rats were housed 2 per cage in filter topped plastic shoe-box style cages in a 12 hr light/dark cycle and fed and watered *ad libitum*. The rats were identified with ear tags, placed at least 1 week prior to the start of the study. Cage cards labeled with animal number, test article, treatment, study number and Institutional Animal Care and Use Committee (IACUC) protocol

number were affixed to the cages. All procedures were reviewed by the Centocor R&D Institutional Animal Care and Use Committee and were conducted in an American Association for Laboratory Animal Care (AALAC) approved facility.

4.3 Data Set

To study the pharmacodynamics of the drugs, rats (5-6/group) received a single s.c. dose of the test articles. Epoetin-α was administered at doses of 0.003, 0.01, 0.03, 0.1 and 0.3 mg/kg. Darbepoetin-α was administered at doses of 0.001, 0.003, 0.01, 0.03, 0.1 and 0.3 mg/kg. CNTO 530 was administered at doses of 0.01, 0.03, 0.1, 0.3 and 1 mg/kg. Control rats received a 10 ml/kg s.c. dose of saline. Blood samples were collected 3, 7, 14, 22, 29, 36, 43, 58 and 71 days after dosing from the retro-orbital sinus under CO_2 anesthesia and whole blood was analyzed with an Advia 120 hematology analyzer (Siemens, Terrytown, NY) as described previously (Kliwinski et al., 2010). Data were collected from 3 separate experiments. The actual day of blood collection was in some cases $\pm$ 1 day from that shown above. The actual day of collection was used for modeling.

To study the pharmacokinetics of CNTO 530, rats were administrated a single s.c. dose of 0.3 mg/kg and blood samples were collected via retro-orbital sinus at 0.3, 1 and 6 hrs and 1, 2, 3, 5, 9, 14, 20 and 27 days after dosing (4 rats per time point) and plasma concentration measured as described previously (Martin et al., 2010). PK values for epoetin-α and darbepoetin-α were obtained from the literature (Woo et al., 2006; Yoshioka et al., 2007). Linear pharmacokinetics were assumed for all three agents.

4.4 Data Analysis

We fit the PK data to Eq. 3.1–3.3 and identified compartmental model parameters for each drug. Then we performed non-compartmental analysis (NCA) on both the observed data and the predicted data from the PK model using PKSolver (Zhang et al., 2010). NCA is a set of statistical methods frequently used to study pharmacokinetics of drugs. It assumes no model structure and uses simple calculations (DiPiro et al., 2005). We then evaluated how well NCA agreed with results of the compartmental PK model. Once we were satisfied with this analysis, the two-compartmental PK model parameters were used to predict PK concentration versus time profile for other dose levels. Using the principle of dose proportionality (Gabrielsson and Weiner, 2007; Gibaldi and Perrier, 1982), the concentration versus time profiles were then used in our PD model.

In analyzing our PD data, we observed that drug responses at some low dosage levels did not differ from control data. So we assumed that the drugs at dosage levels did not induce biologically significant responses. Based on these observations, we used RBC counts from the control rats to calculate a normal range with 95% confidence interval (mean $\pm$ 1.96 standard deviation (SD)). If more than 95% of RBC counts in rats with a certain dosage level fall into that range, we did not use that dosage level for the drug in our analysis. As a result, we excluded epoetin-α at two lowest dosage levels (0.003 mg/kg and 0.01 mg/kg), darbepoetin-α at the lowest dosage levels (0.001 mg/kg) and CNTO 530 at two lowest dosage levels (0.01 mg/kg and 0.03 mg/kg). This gave us a data set of 78 rats. We applied our PD model to the

merged dataset. The time points of RET and RBC for all dose levels of each drug were analyzed simultaneously with predicted PK profiles. The expected HGB levels were calculated using Eq. 3.16.

Both PK and PD model fittings were done by maximum likelihood (ML) method, which is available as a computation option in the ADAPT II software package (D'Argenio and Schumitzky, 1997). The basic idea of ML is to select parameter values to maximize a preset maximum likelihood function (Le Cam, 1990). Since this software requires a variance model, we incorporated the following relationship:

$$V_i = (\sigma_{inter} + \sigma_{slope} \times Y_i)^2 \tag{4.1}$$

where V_i is the variance at the ith data point, σ_{inter} and σ_{slope} are the variance model parameters, and Y_i represents the model predicted value at the ith time point. For example, we assume that $\sigma_{inter} = 0.2$ and $\sigma_{slope} = 0.1$ in Eq. 4.1. Then the variance model represents an error process with a standard deviation of 0.2 plus 10% of the measured quantity.

4.5 Results

4.5.1 PK model results

The concentration values at each time point of three drugs are shown in Figures 4.1–4.3. We fit the mean values of the concentration data for each drug to our model using the bioavailability, F, values of 0.59 for epoetin-α (Woo et al., 2006), 0.54 for darbepoetin-α (Yoshioka et al., 2007), and 0.75 for CNTO 530 from our experiments.

The predicted concentration versus time profiles are shown in Figures 4.1–4.3 as solid lines. To evaluate the PK model, we calculated non-compartmental parameters from model predictions and compared them with those calculated from experimental data. As shown in Table 4.1, the results from the PK model are within or close to mean ± SD of the results of NCA from experimental data. This indicates that our PK model is a good prediction of concentration versus time profiles.

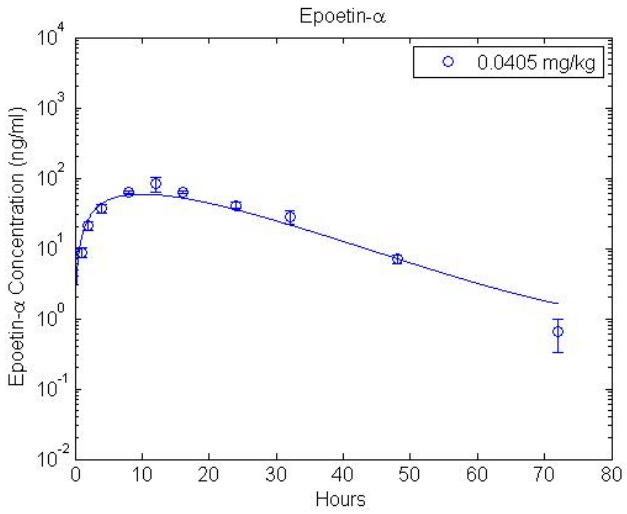

Figure 4.1: Epoetin-α concentration versus time profile (0.0405 mg/kg) estimated from experimental data provided by Woo et al. (2006).

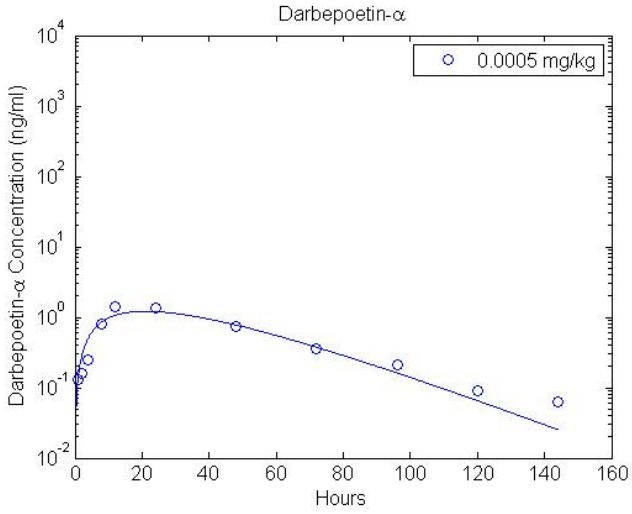

Figure 4.2: Darbepoetin-α concentration versus time profile (0.0005 mg/kg) estimated from experimental data provided by Yoshioka et al. (2007).

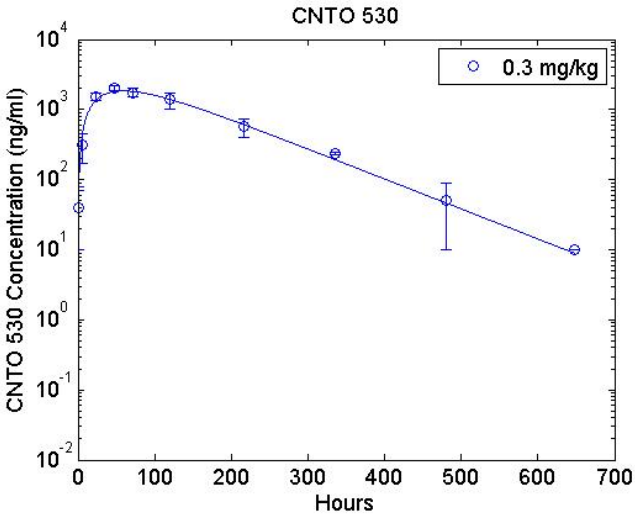

Figure 4.3: CNTO 530 concentration versus time profile (0.3 mg/kg) estimated from our PK experiment.

Table 4.1: Non-compartmental analysis for epoetin-α, darbepoetin-α and CNTO 530.

Parameters	**Definition**	**Epoetin-α** (0.0405 mg/kg)		**Darbepoetin-α** (0.0005 mg/kg)		**CNTO 530** (0.3 mg/kg)	
		From data[a]	From prediction[b]	From data[c]	From prediction[b]	From data[a]	From prediction[b]
AUC_{0-inf} (ng.h/ml)	Area under the curve	1920.00 ± 118.40	2064.66	74.12 ± 5.6	70.01	350249 ± 33957	336367
C_{max} (ng/ml)	Maximal concentration	83.68 ± 18.34	66.94	1.36 ± 0.99	1.21	2062 ± 164	1843
T_{max} (h)	Time that C_{max} occurs	12.2 ± 1.72	11.27	15 ± 6	21.82	54.86 ± 17.18	58.91
$T_{1/2}$ (h)	Terminal half life	7.76 ± 0.9	9.73	15.09 ± 0.48	17.92	72.47 ± 5.42	70.34
CL/F (ml/h/kg)	Apparent total clearance	21.16 ± 1.29	19.62	6.8 ± 0.5	7.18	0.86 ± 0.08	0.89

[a]is expressed as mean ± SD that were calculated from 2000 simulation based on data time points
[b]is expressed as values that were calculated from predicted curves of PK model
[c]is taken from literature (Yoshioka et al., 2007)

We plotted predicted concentration profiles for all three drugs at a dosage level of 0.3 mg/kg (Figure 4.4). The plot suggests that at the same dosage, epoetin-α concentration profile has the lowest peak and shortest active time; CNTO 530 has the highest peak and longest active time.

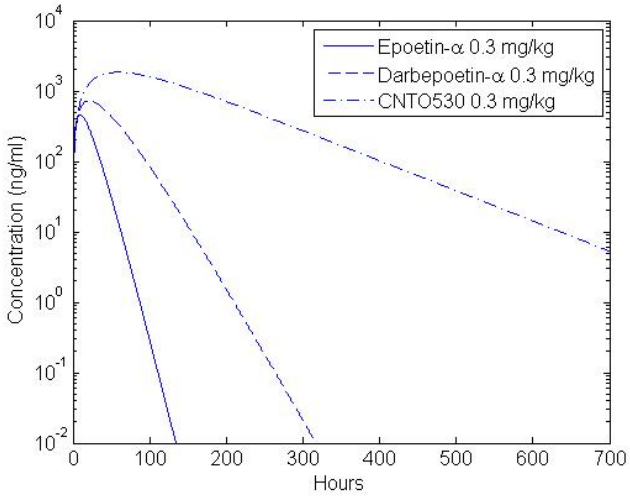

Figure 4.4: Predicted concentration of all three ESAs at a dosage level of 0.3 mg/kg.

The estimated PK model parameters were listed in Table 4.2. In our study, we found that the estimated elimination rates (K_{el}), volume of distribution (V_C) and absorbtion rate (K_a) are highest for epoetin-α, and lowest for CNTO 530. The relatively slow rate of decrease of CNTO 530 concentration shown in Figure 4.3 is likely due to the fact that CNTO 530 has lower absorption and elimination rates than the other two ESAs. The estimated values for inter-compartmental rate (K_{CP}) are close to 0 for epoetin-α and darbepoetin-α. This implies that one compartmental PK model might also work for these two drugs. However, K_{CP} for CNTO 530 is 0.01 h^{-1}, which implies that two-compartmental PK model should work better for CNTO 530. This reinforces our choice of using a two-compartmental PK model for all three

drugs.

Table 4.2: Estimated PK parameters for all three ESAs using our model.

Parameters	Definition	**Epoetin-α**	**Darbepoetin-α**	**CNTO 530**
K_{el} (h^{-1})	Elimination rate	0.11	0.05	0.01
V_c (ml/kg)	Volume of distribution of central compartment	142.6	82.33	67.28
K_a (h^{-1})	Absorption rate	0.11	0.05	0.03
K_{CP} (h^{-1})	Inter-compartment rate from central to peripheral	$\sim$0.00	$\sim$0.00	0.01
K_{PC} (h^{-1})	Inter-compartment rate from peripheral to central	0.61	1.93	0.87

4.5.2 PD model results

Our experimental data time span is up to 72 days (1728 hours). Other studies in the literature did not exceed 60 days (Agoram et al., 2006; Loeffler et al., 1989; Ramakrishnan et al., 2004; Wichmann et al., 1989; Woo et al., 2006; Wulff et al., 1989) and thus their models have difficulty fitting our data. For example, when we implemented Woo et al.'s model, we found that RET counts were suddenly increased and RBC counts suddenly dropped after 1440 hours (see Figure 4.5), which is inconsistent with actual responses. Hence, we designed our PD model to incorporate a longer time span.

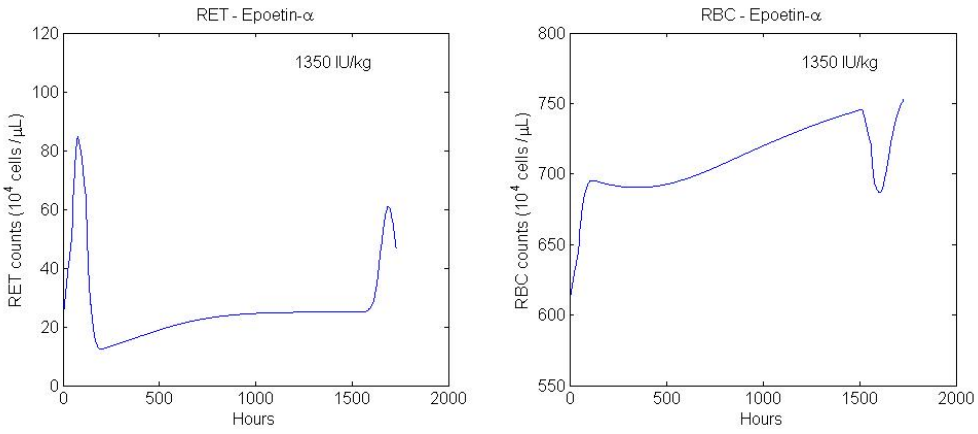

Figure 4.5: We implemented the PK/PD model in Woo et al. (2006) at a dose 1350 IU/kg (0.0135 mg/kg) and ran an extended simulation that went to 1728 hours (72 days). A significant inconsistency in the model can be seen in the plots of RET and RBC after 1440 hours (60 days).

The plots of the measured data and the predicted curves from our PD model for the three ESAs are shown in Figures 4.6–4.8. The RET, RBC and HGB profiles for all three drugs share the same characteristics. Each profile quickly increases a short time after dosing, then decreases to below the baseline and eventually recovers back to the initial level. These results suggest that our PD model fits the response data

of all three ESAs with reasonable accuracy and allows us to study drug effects over a longer time span (up to 72 days) than previous models.

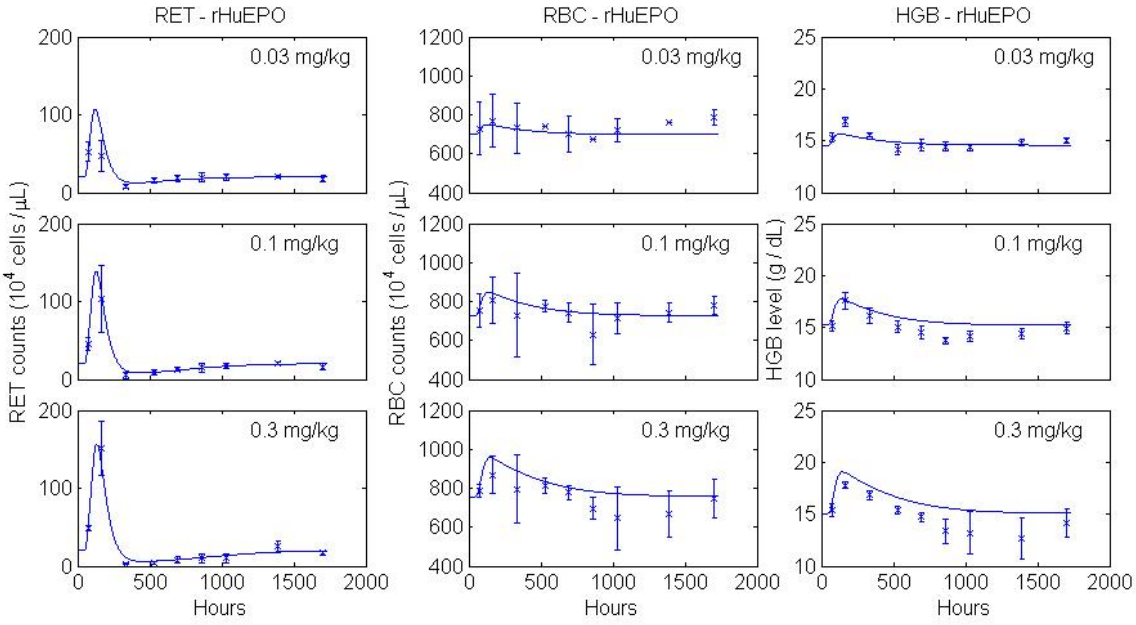

Figure 4.6: The plots of the experimental data (RET, RBC and HGB) and their model predicted curves from our PD model for epoetin-α.

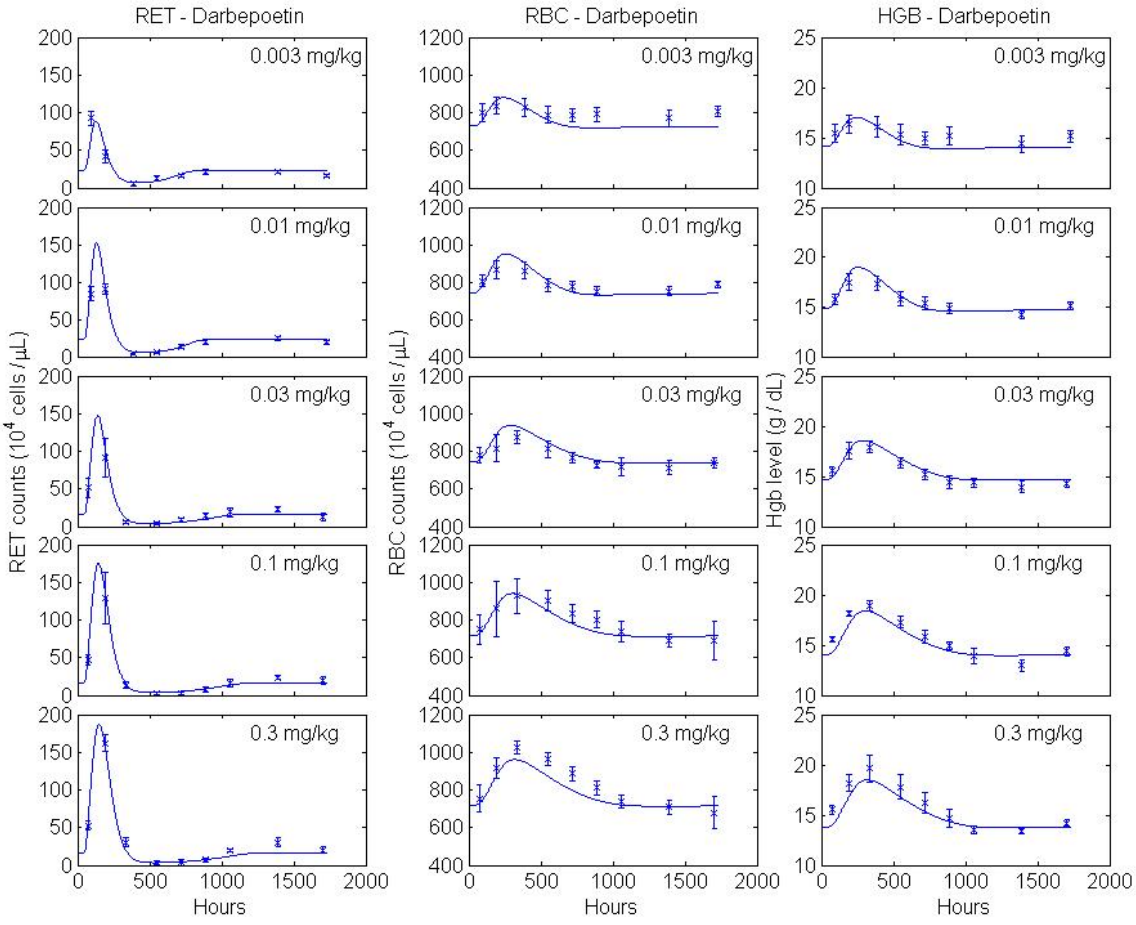

Figure 4.7: The plots of the experimental data (RET, RBC and HGB) and their model predicted curves from our PD model for darbepoetin-α.

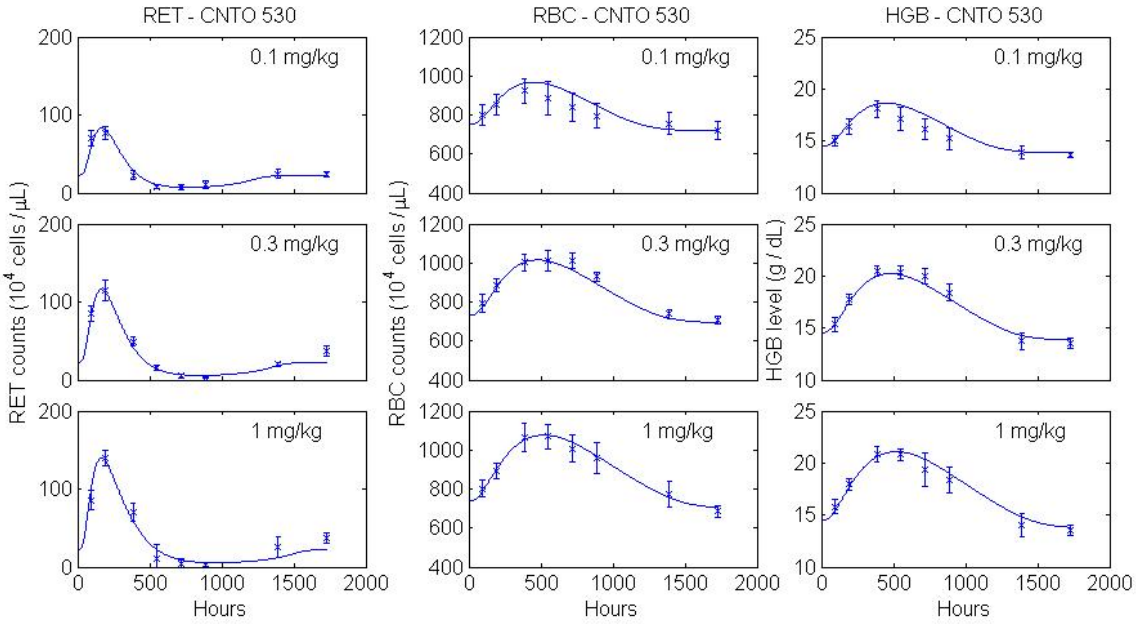

Figure 4.8: The plots of the experimental data (RET, RBC and HGB) and their model predicted curves from our PD model for CNTO 530.

The goodness-of-fit plots of our PD model are shown in Figures 4.9–4.11. For darbepoetin-α and CNTO 530, the observed versus predicted values for RET, RBC and HGB fell along the line of unity, indicating that the PD model describes the data reasonably well. For epoetin-α, the goodness-of-fit plots for RET, RBC and HGB have some points much lower than the line of unity. This suggests that epoetin-α data have a large variance (see Figure 4.6) and thus the PD model parameters also have a large variance.

The estimated parameters for our PD model are listed in Table 4.3. To enable direct comparison of the parameters, we normalized each PD model parameter by dividing it by the mean value over all three ESAs and plotted them in Figure 4.12 (Krzyzanski et al., 2005). We see that T_{RET} (lifespan of reticulocytes), S_{max} (maximum stimulatory effect), $1/K_e$ (time to change $K_{in}(t)$), and IC_{50} (potency of

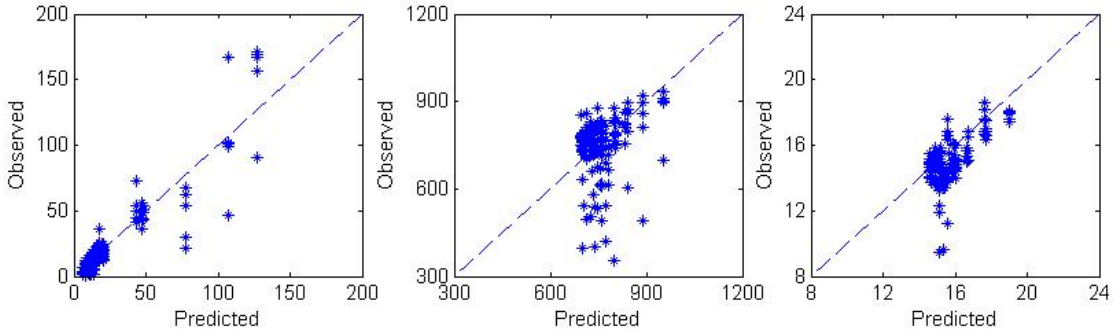

Figure 4.9: Goodness-of-fit of RET, RBC and HGB for PD modeling of epoetin-α.

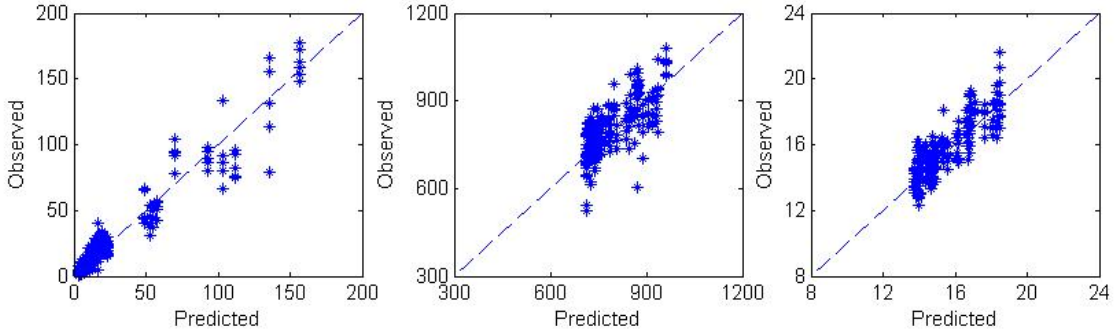

Figure 4.10: Goodness-of-fit of RET, RBC and HGB for PD modeling of darbepoetin-α.

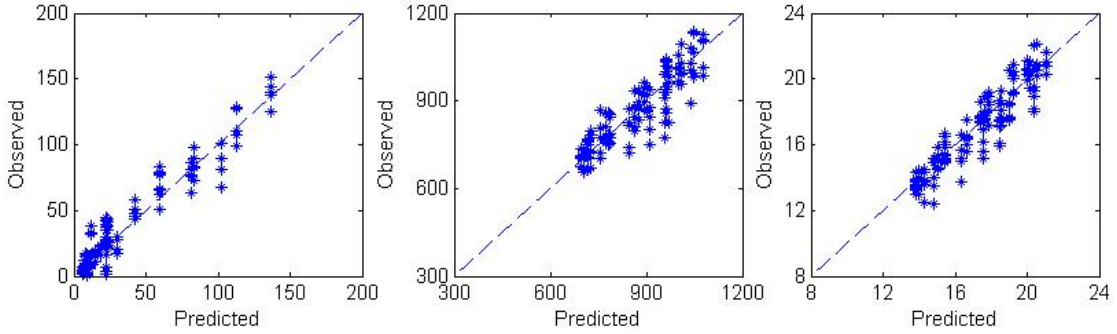

Figure 4.11: Goodness-of-fit of RET, RBC and HGB for PD modeling of CNTO 530.

inhibitory effect) are statistically similar for all three ESAs. The mean value of T_d (time to mobilize reticulocytes and RBCs) for epoetin-α (50.14 h) and darbepoetin-α (46.24 h) are similar, but higher than the other two ESAs. Also, the potency value (SC_{50}) for CNTO 530 is significantly different than it is for epoetin-α or darbepoetin-α (see Figure 4.12) suggesting that a larger CNTO 530 concentration is required to reach the same stimulation effect for RBCs than for epoetin-α or darbepoetin-α.

Table 4.3: Estimated PD parameters for all three ESAs using our model.

Parameters	[a]**Epoetin-α**		[b]**Darbepoetin-α**		[c]**CNTO 530**	
	Mean	[d]CV(%)	Mean	CV(%)	Mean	CV(%)
T_{RET}	31.70	269	25.08	38	44.16	28
T_d (h)	50.14	32	46.24	7	18.65	39
$1/K_e$ (h)	49.20	134	47.12	17	78.64	32
S_{max}	13.27	82	15.42	10	12.04	21
SC_{50} (ng/ml)	7.39	241	12.31	20	710.4	33
IC_{50} (g/dl)	0.97	135	0.97	18	1.32	32

Note:
[a]: used doses of 0.03 mg/kg, 0.1 mg/kg, and 0.3 mg/kg
[b]: used doses of 0.003 mg/kg, 0.01 mg/kg, 0.03 mg/kg, 0.1 mg/kg, and 0.3 mg/kg
[c]: used doses of 0.1 mg/kg, 0.3 mg/kg, and 1 mg/kg
[d]: stands for coefficient of variation expressed as SD/mean

Figure 4.13 shows $E(t)$, the combined stimulation/inhibition effect, for the three drugs all at the same dosage of 0.1 mg/kg. We observed that the curves of $E(t)$ decreased quickly a short time after dosing, then increased above the baseline and returned gradually to the baseline. The plots suggest that there is a combination of stimulation and inhibition which affects the conversion of reticulocytes into mature RBCs.

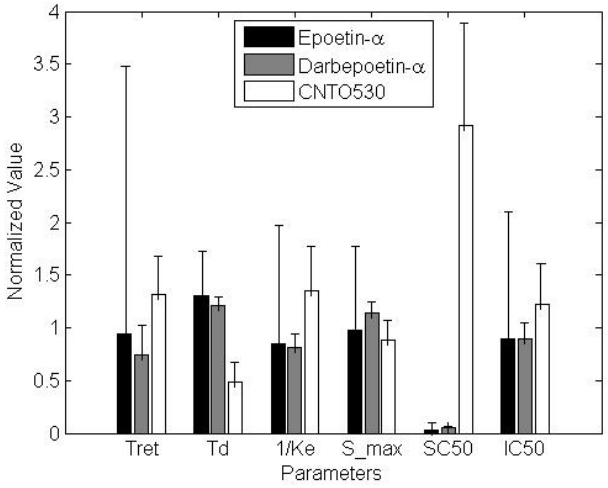

Figure 4.12: Means and SDs of the normalized estimates of the PD parameters for all three ESAs.

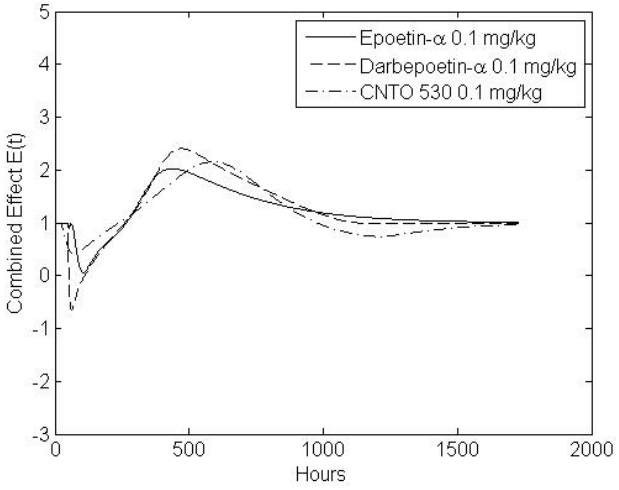

Figure 4.13: E(t) for all three ESAs with dosage 0.1 mg/kg.

4.6 Discussion

Typical PK/PD models from the literature (Ette and Williams, 2007; Ramakrishnan et al., 2003; Woo and Jusko, 2007) use compartmental structures where various pools represent ESA concentrations or cell populations at different stages or conditions. In PK modeling, both one-compartmental and two-compartmental models have been used (Krzyzanski and Jusko, 1998; McLennan et al., 2006). They can be mathematically expressed using linear differential equations (Agoram et al., 2006) or non-linear differential equations (Woo and Jusko, 2007). In PD modeling, indirect response models and cell lifespan models were developed to analyze the dynamics of erythropoietic responses, such as reticulocyte (RET) counts, red blood cell (RBC) counts, and hemoglobin (HGB) levels. In 1993, Dayneka et al. proposed four basic models for characterizing indirect PD responses with differential equations and Hill functions, which have been widely used in studying the pharmacodynamics of ESAs. Krzyzanski et al. (2005) developed a PK/PD model for epoetin-α after multiple s.c. doses in healthy human populations, where catenary cell production and cell lifespan concepts (Krzyzanski et al., 1999) were used to fit the RET percentages, RBC counts and HGB levels. Their PD model combined first-order loss rates and life span delayed loss rates. However, they did not include inhibitory effects in their model. Woo et al. (2006) developed a PK/PD model for epoetin-α in rats where they incorporated cell lifespan loss concept and indirect response to ESAs. Unlike Krzyzanski, Woo's model included an inhibition feedback from hemoglobin. The lifespan of RBC in their PD model was assumed to be 60 days (1440 hours) and their experimental

data were collected within 24 days (576 hours) of epoetin-α administration. When we attempted to implement their model for data collected more than 60 days after epoetin-α administration, we found that these data are not well modeled due to the cell lifespan loss concept in the model. This concept introduces a significant decline of RBC counts after 60 days, which is not biologically reasonable. Hence, the lifespan loss concept was inappropriate for modeling long-term erythropoietic responses, such as the RBC count after 60 days. Similarly, Agoram et al. (2006) developed a PK/PD model of darbepoetin-α in humans. When we implemented this model and tested it with our data, we found that this PD model could not capture the "below the baseline" phenomenon in hemoglobin data observed after 60 days.

Pharmacokinetic models of ESAs have also been extensively studied in the literature (Agoram et al., 2006; Ette and Williams, 2007; Khorasheh et al., 1999). After testing various model structures we found that a simple linear two-compartmental PK model is applicable to all three drugs in our study. We developed a new indirect response PD model, which included negative feedbacks and effectively described drug response data of all three drugs in our study. We used a variable to model the production rate change of RET and introduced a joint regulatory effect $E(t)$ controlled by the drug concentration and HGB level, which regulates how RETs become mature RBCs. The variable production rate helps to better model drug effects in the initial stages after administration. The feedback mechanism provided by I(t) and $E(t)$ caused the response curve to decrease below baseline and then gradually return to the normal levels mimicking experimental results.

Our PD model fit the experimental data and showed similar trends in the time

profiles for RET counts, RBC counts and HGB levels for all three drugs. RET counts increased shortly after dosing, reached a peak, and then decreased. This decrease in RET counts continued below baseline values and then gradually returned back to the baseline. This observation was also reported in the literature (Ramakrishnan et al., 2004; Woo et al., 2006). For RBC and HGB, the trends are similar. For epoetin-α, unlike for darbepoetin-α and CNTO 530, the RBC count does not change significantly after administration even at a high dose level.

The development of a single PK/PD model for all three drugs allows parameter comparisons between ESAs to be easily made. It is shown in Table 4.2 and 4.3 that the PK/PD parameters of epoetin-α and darbepoetin-α are more similar to each other than they are to CNTO 530. Compared to epoetin-α and darbepoetin-α, CNTO 530 provides the advantage of longer half life ($t_{1/2}$) and shorter mobilization time (T_d), which indicates that it mobilizes reticulocytes and RBCs faster and the stimulatory effect lasts longer. However, CNTO 530 has a much larger SC_{50} (less potency), which means it requires a larger drug concentration to reach the same stimulation effect for RBCs provided by either epoetin-α or darbepoetin-α. From Figure 4.8, it is clear that CNTO 530 has the highest peak and stays above the baseline the longest. This suggests that for CNTO 530 the stimulation of RBC generation gives it a clear advantage over epoetin-α and darbepoetin-α despite relatively less potency (SC_{50}).

4.7 Conclusion

We developed a single PK/PD model for three ESAs. The PK model is an existing linear two-compartmental model (DiPiro et al., 2005). The new PD model is an

indirect response model that includes several negative feedbacks and fits response data for up to 72 days. When comparing among the erythropoietic responses to doses that increased RBC, the coefficients of the model indicate that despite having a lower potency, CNTO 530 caused a more rapid mobilization of RET. The results of the PK/PD modeling suggest that CNTO 530 stimulates erythropoiesis in a similar fashion to epoetin-α and darbepoetin-α and that the PK properties of an ESA are the most important factor in determining efficacy.

Chapter 5: An Application of PK/PD modeling: Dose Threshold Study

5.1 Introduction

Pharmaceutical compounds are known to have a dose threshold below which they do not have a "significant" effect on a specific biological process (Eaton and Kalaassen, 1996). The determination of what is "significant" and which specific biological process is to be targeted affects the value of the dose threshold. For instance, in the treatment of anemia the biological process of interest is erythropoiesis and a drug with dose exceeding a certain threshold has a "significant" effect if it causes a noticeable increase in red blood cell counts above baseline. The key benefit of knowing the dose threshold is that a dose which is slightly above the dose threshold (minimum effective dose) can be administered. By prescribing an appropriate dosage, side effects of the compound may be diminished and costs of treatment may be reduced.

In many cases the effectiveness of a pharmaceutical compound is determined by non-quantitative analysis of experimental data (Braga et al., 1999; Reigner et al., 2003; Sathyanarayana et al., 2009). This type of subjective analysis is prone to errors in estimating the drug threshold due to differences in opinion between professionals. We suggest two approaches to improve this situation. One is based on the assumption that when a dose is below threshold the pharmacodynamic response is constant (within some "small" distance from baseline). Conversely when a dose is above threshold the pharmacodynamic response has a "significant" number of readings which are

not within a "small" distance from baseline. The second approach assumes a good PK/PD model. The experimental drug responses at doses above the threshold should agree with the model prediction much better than at doses below the threshold.

In the first approach, we calculate a normal range with a certain confidence interval using data from control subjects. Then we determine how many drug response data points fall in the range. If the number is large, the response profile does not differ from control; thus the corresponding dosage is below the threshold. Otherwise, the dosage is above threshold.

In the second approach, we used our existing PK/PD model to predict drug responses at each dosage and applied R^2, coefficient of determination, to measure how well the prediction agrees with experimental data. If R^2 is significantly small, we say the corresponding dose is below threshold and if R^2 is large, we say the dose is above threshold.

5.2 Experimental Data and Data Analysis

The hematology data used in the dose threshold study consisted of blood samples from sixty three rats. The rats were evenly subdivided into nine groups. One of the groups was a control group while the other eight groups were each subcutaneously administered with a different dose of CNTO530. The dosage levels used for each of the eight groups were 0.005 mg/kg, 0.01 mg/kg, 0.02 mg/kg, 0.04 mg/kg, 0.08 mg/kg, 0.16 mg/kg, 0.32 mg/kg, and 1 mg/kg. For each group blood samples were drawn from all rats at day 3, 9, 16, 23, 30, 37, 57, and 72 after administration. For each blood sample reticulocyte count (RET), red blood cell count (RBC), and the

hemoglobin level (HGB) were obtained using an Advia 120 hematology analyzer.

5.3 Two Criteria

The following method was used to find the dosage levels at which the drug response data were not significant from the control data. All RBC counts from the control rats were used to calculate a normal range with 95% confidence interval (mean $\pm$1.96 SD). If more than 95% of RBC counts of the drug at a specific dosage level fell into that range, we considered the dosage level below the threshold, i.e. the drug response profile is flat and the drug fails to cause a statistically noticeable change. Conversely, if less than 95% of RBC counts at a specific dosage level fall into that range, we considered the dosage level above the threshold.

For the second approach to determine dose threshold, we applied our PK/PD model to the experimental CNTO 530 dataset and assessed the model fit using R^2, the coefficient of determination used to quantify goodness of fit. Its definition is as follows:

$$R^2 = 1 - SSE/SST \tag{5.1}$$

where SSE is sum of square of errors between observations and predicted points and SST is sum of square of errors from observations to the mean of observations (a horizontal line). A higher value of R^2 indicates that the model fits the data better. When R^2=1.0, all points lie exactly on the curve with no scatter. When $R^2 = 0.0$, the best-fit curve fits the data no better than a horizontal line going through the mean of all Y values. R^2 can be negative, if the best-fit curve fits the data even worse than

does a horizontal line.

5.4 Results

We analyzed drug response data at eight dosage levels using the 95% criterion. The four lowest dosage levels (0.005 mg/kg, 0.01 mg/kg, 0.02 mg/kg, and 0.04 mg/kg) were found to be below the threshold. The remaining four dosage levels (0.08 mg/kg, 0.16 mg/kg, 0.32 mg/kg and 1 mg/kg) were found to be above the threshold and able to induce detectable drug response.

We calculated the percentage of RBC counts within the normal range for each of eight dosages and show them in Table 5.1. For each drug, there are 7 rats and each rat was sampled at 8 different time points. So there are maximum 56 time points. However, there are fewer usable time points for some dosages because some samples were clotted or some rats were sacrificed before the end of our study.

Table 5.1: Percentage of RBC counts within the normal range of CNTO 530.

Dosage level of CNTO 530	Number of RBC counts within the normal range	Total Usable Time Points	% of RBC counts within the normal range
0.005 mg/kg	54	54	100
0.01 mg/kg	54	54	100
0.02 mg/kg	53	54	98
0.04 mg/kg	53	54	98
0.08 mg/kg	46	56	82
0.16 mg/kg	35	55	64
0.32 mg/kg	19	56	34
1 mg/kg	13	55	24

We then applied our PD model to predict drug response data. The model fitting

plots for RET, RBC and HGB at the eight dosage levels of CNTO 530 are shown in Figure 5.1–5.3. These plots share the same characteristics. For each plot, we see a quick increases in the variable after a short delay, then a decrease to below baseline, and a slow recover to the initial level. This trend was also reported in previous PK/PD studies (Ramakrishnan et al., 2004; Woo et al., 2006). From these figures, it is clear that our PD model fit the data well for the highest four dosage levels. Additionally, for the highest four dosage levels, the model predictions and observed data for RETs, RBCs and HGBs fell along the line of unity (See Figure 5.4), which indicates that the model fit the drug response data well at 0.08, 0.16, 0.32 and 1 mg/kg.

The coefficients of determination R^2 are shown both in Figures 5.1–5.3 and in Table 5.2. For the lowest four dosage levels, R^2 values for RET, RBC and HGB are either relatively small (< 0.1) or negative except for RET at 0.04 mg/kg. When R^2 for RET prediction is about 0.5 but negative for both RBC and HGB. This may indicate that this dosage is close to the threshold, showing mixed model prediction results. For the highest four dosage levels, R^2 values for RET, RBC and HGB are quite large, indicating that our PD model describes the data reasonably well. In summary, by measurement of R^2, we were able to verify our finding of dose threshold with the normal range method. This confirms that the dose threshold is between 0.04 mg/kg and 0.08 mg/kg and is consistent with our previous analysis, which suggested the dose threshold should be between 0.03 and 0.1 mg/kg (see Chapter 4).

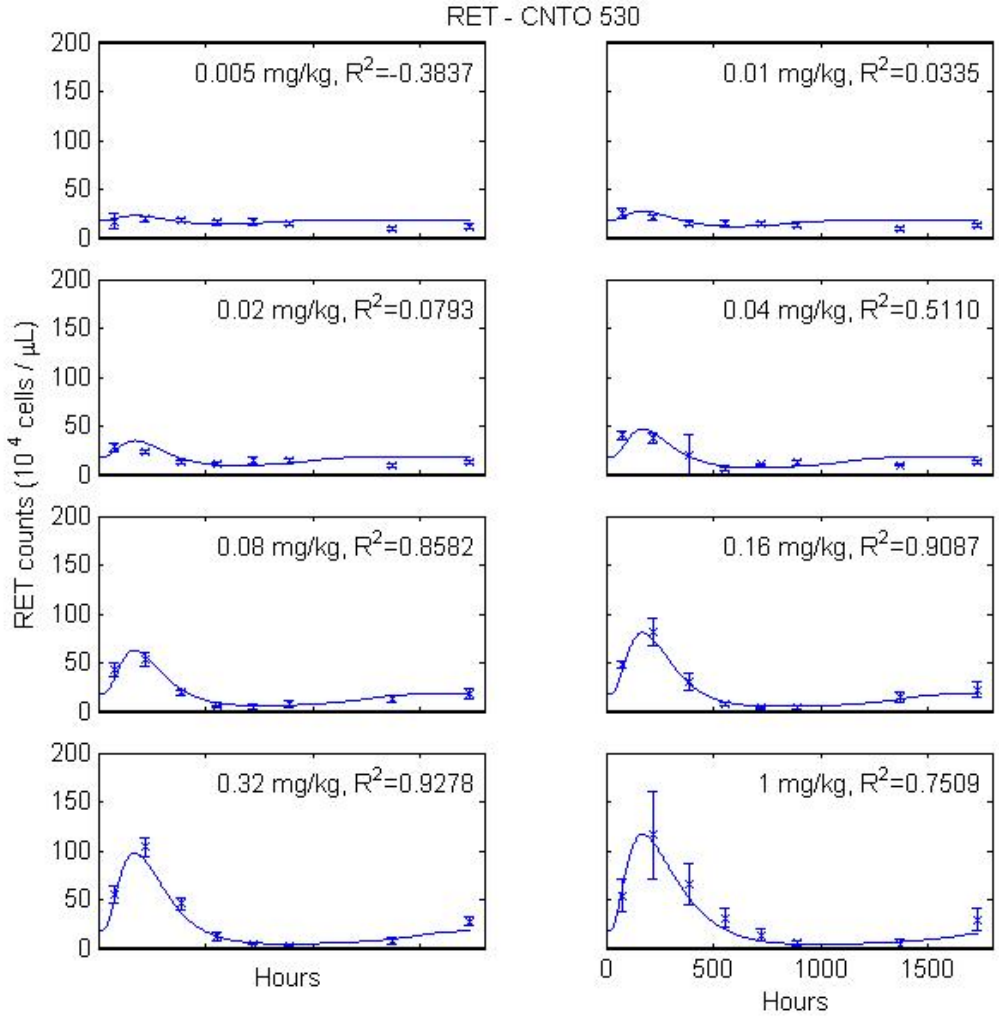

Figure 5.1: RET profiles after s.c. administration of CNTO 530 with dosage levels of 0.005 mg/kg, 0.01 mg/kg, 0.02 mg/kg, 0.04 mg/kg, 0.08 mg/kg, 0.16 mg/kg, 0.32 mg/kg, and 1 mg/kg.

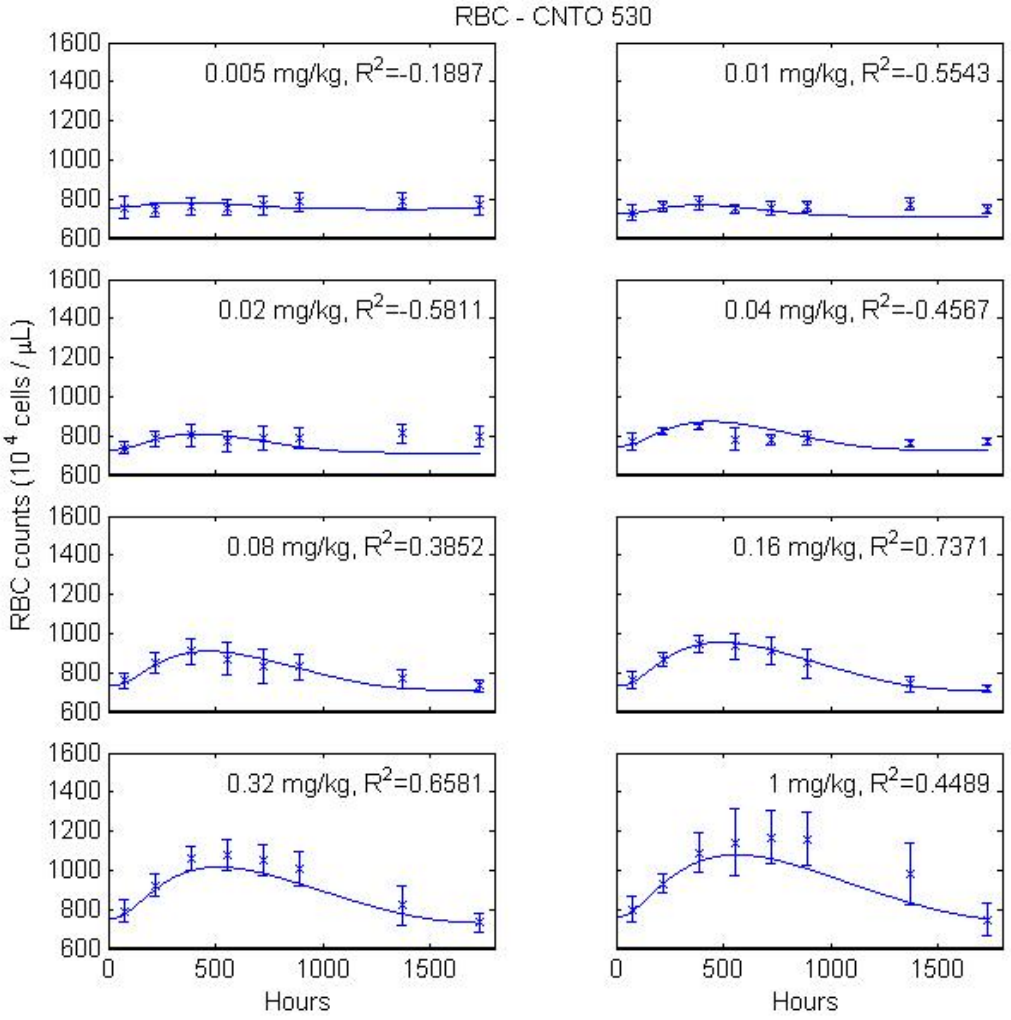

Figure 5.2: RBC profiles after s.c. administration of CNTO 530 with dosage levels of 0.005 mg/kg, 0.01 mg/kg, 0.02 mg/kg, 0.04 mg/kg, 0.08 mg/kg, 0.16 mg/kg, 0.32 mg/kg, and 1 mg/kg.

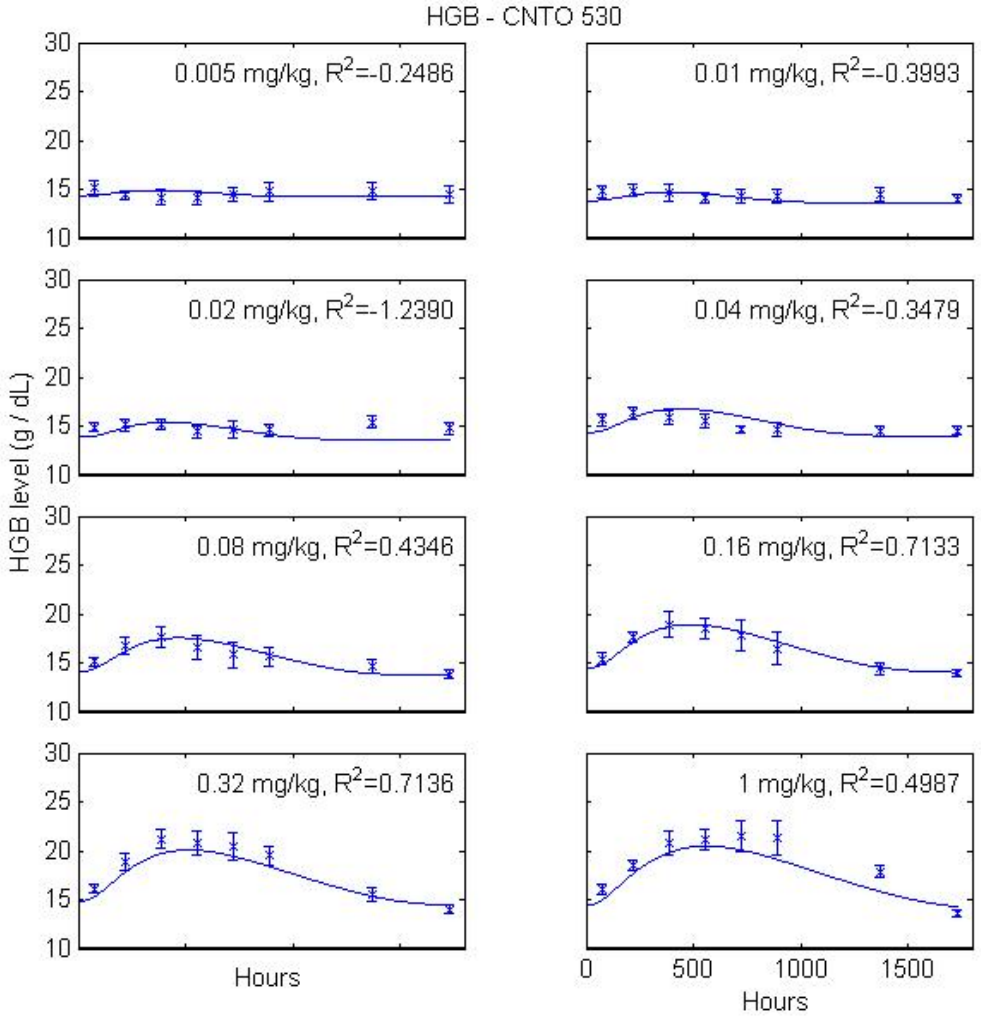

Figure 5.3: HGB profiles after s.c. administration of CNTO 530 with dosage levels of 0.005 mg/kg, 0.01 mg/kg, 0.02 mg/kg, 0.04 mg/kg, 0.08 mg/kg, 0.16 mg/kg, 0.32 mg/kg, and 1 mg/kg.

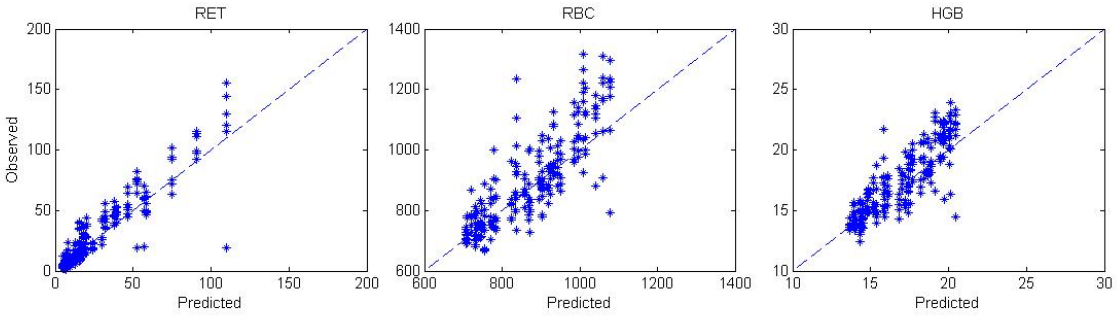

Figure 5.4: Goodness-of-fit of RET, RBC and HGB for PD model predication of CNTO 530 at 0.08, 0.16, 0.32 and 1 mg/kg.

Table 5.2: R^2 calculated from the prediction of drug responses (RET, RBC and HGB) using our model for CNTO 530

Dosage level of CNTO 530	RET	RBC	HGB
0.005 mg/kg	-0.3837	-0.1897	-0.2486
0.01 mg/kg	0.0335	-0.5543	-0.3993
0.02 mg/kg	0.0793	-0.5811	-1.2390
0.04 mg/kg	0.5110	-0.4567	-0.3479
0.08 mg/kg	0.8582	0.3852	0.4346
0.16 mg/kg	0.9087	0.7371	0.7133
0.32 mg/kg	0.9278	0.6581	0.7136
1 mg/kg	0.7509	0.4489	0.4987

5.5 Discussion

The identification of drug effect threshold depends on the type of response that is measured and can vary among individuals. Even so, it is important to know the dosages at which there is no detectable drug effect and to determine thresholds on minimum effective dose. Using the minimum effective dose can help reduce the amount and consequently the toxicity and cost of the therapy (Braga et al., 1999).

Based on our analysis in this chapter and our development of the PK/PD model, we showed that the dosage threshold for single dose administration of CNTO 530 in rats is between 0.04 mg/kg and 0.08 mg/kg. These methods can help scientists to find dosage threshold for other pharmaceutical compounds during the process of drug development and for physicians to prescribe appropriate doses of medications for patients.

Chapter 6: Summary and Future Work

6.1 Summary of Thesis

In this thesis, we developed a single PK/PD model for three ESAs: epoetin-α, darbepoetin-α and CNTO 530. We found that a classical two-compartmental PK model from the literature (DiPiro et al., 2005) can be applied to our data. However, it was discovered that the available PD models were not able to adequately describe our data. So we developed a new indirect response model. Instead of using a constant as in previous studies, we used a variable to model the production rate of RET and introduced a joint regulatory effect $E(t)$ which is controlled by both drug concentration and change in hemoglobin level. This joint effect $E(t)$ regulates how RET become mature RBC. Applying our PK/PD model to the experimental data of the three drugs, we obtained their model parameters, which make a meaningful comparison possible. After carefully comparing the parameters, we found that the drug action of CNTO 530 is significantly different from the other two drugs.

Next, we developed two statistical criteria to identify dose threshold of a drug. For the first criterion, by computing how many data points in a drug experiment are in the 95% confidence interval of control data, we can determine minimum effective drug doses. For the second one, we used R^2 to measure and compare the fitting of PK/PD models under different doses and determine effective doses. When we applied our methods to the CNTO 530 data set, we got very similar results, suggesting their

validity.

6.2 Future Work

- **Test our PK/PD model with more dosage data**

  Our PK/PD model was fitted and tested with data from three ESAs, epoetin-α, darbepoetin-α and CNTO 530 over a dose range of 0.001 mg/kg to 1mg/kg. The model can be tested at higher dose levels to determine its validity over a much wider range of treatments.

- **Improve PD model**

  A more accurate PD model may be developed by expanding the "Early Stages" compartment in our model. This could include data on BFU-E, CFU-E, Pro-EB, Baso-EB, Poly-EB and Ortho-EB. Although this will complicate our model we will have a more precise picture of RBC_M production.

Bibliography

B. Agoram, A. C. Heatherington, and M. R. Gastonguay. Development and evaluation of a population pharmacokinetic-pharmacodynamic model of darbepoetin alfa in patients with nonmyeloid malignancies undergoing multicycle chemotherapy. *AAPS J*, 8(3):E552–63, 2006.

M. Braga, L. Gianotti, O. Gentilini, A. Vignali, L. Corizia, and V. Di Carlo. Erythropoiesis after therapy with recombinant human erythropoietin: a dose-response study in anemic cancer surgery patients. *Vox Sang*, 76(1):38–42, 1999.

P. J. Bugelski, T. Nesspor, A. Volk, J. O'Brien, D. Makropoulos, K. Shamberger, P. W. Fisher, I. James, D. Graden, and R. J. Capocasale. Pharmacodynamics of recombinant human erythropoietin in murine bone marrow. *Pharm Res*, 25(2): 369–78, 2007.

P. J. Bugelski, R. J. Capocasale, D. Makropoulos, D. Marshall, P. W. Fisher, J. Lu, R. Achuthanandam, T. Spinka-Doms, D. Kwok, D. Graden, A. Volk, T. Nesspor, I. E. James, and C. Huang. Cnto 530: molecular pharmacology in human ut-7epo cells and pharmacokinetics and pharmacodynamics in mice. *J Biotechnol*, 134(1-2): 171–80, 2008.

Peter Bugelski. Introduction to erythropoiesis and cnto 530. Technical report, 2005.

H. F. Bunn. New agents that stimulate erythropoiesis. *Blood*, 109(3):868–73, 2007.

W Cheung, D Gibson, C Cote, and E Vereammen. Pharmacokinetic and pharmacodynamic modeling of erythropoietin administration, 2004.

W. K. Cheung, B. L. Goon, M. C. Guilfoyle, and M. C. Wacholtz. Pharmacokinetics and pharmacodynamics of recombinant human erythropoietin after single and multiple subcutaneous doses to healthy subjects. *Clin Pharmacol Ther*, 64(4):412–23, 1998.

Daan Crommelin, Robert Sindelar, and Bernd Meibohm. *Pharmaceutical Biotechnology: Fundamentals and Applications.* Informa healtcare USA, third edition, 2008.

DZ D'Argenio and A Schumitzky. Adpt ii user's guide: Pharmacokinetic/pharmacodynamic system analysis software. Technical report, Biomedical Simulations Resource, 1997.

N. L. Dayneka, V. Garg, and W. J. Jusko. Comparison of four basic models of indirect pharmacodynamic responses. *J Pharmacokinet Biopharm*, 21(4):457–78, 1993.

H. Derendorf and B. Meibohm. Modeling of pharmacokinetic/pharmacodynamic (pk/pd) relationships: concepts and perspectives. *Pharm Res*, 16(2):176–85, 1999.

Joseph T. DiPiro, William J. Spruill, Robert A. Blouin, Jane M. Pruemer, and William E. Wade. *Concepts in Clinical Pharmacokinetics*. ASHP, Bethesda, 4 edition, 2005.

DL Eaton and CD Kalaassen. *Principles of ftoxicology. In Casarett & Doulls' toxicology: The basice science of poisons*. McGraw-Hill, New York, 5 edition, 1996.

J. C. Egrie and J. K. Browne. Development and characterization of novel erythropoiesis stimulating protein (nesp). *Nephrol Dial Transplant*, 16 Suppl 3:3–13, 2001.

J. C. Egrie, T. W. Strickland, J. Lane, K. Aoki, A. M. Cohen, R. Smalling, G. Trail, F. K. Lin, J. K. Browne, and D. K. Hines. Characterization and biological effects of recombinant human erythropoietin. *Immunobiology*, 172(3-5):213–24, 1986.

J. C. Egrie, E. Dwyer, J. K. Browne, A. Hitz, and M. A. Lykos. Darbepoetin alfa has a longer circulating half-life and greater in vivo potency than recombinant human erythropoietin. *Exp Hematol*, 31(4):290–9, 2003.

E. I. Ette and P. J. Williams. *Pharmacometrics: the science of quantitative pharmacology*. John Wiley and Sons Inc., Hoboken, NJ, 2007.

D. Faulds and E. M. Sorkin. Epoetin (recombinant human erythropoietin). a review of its pharmacodynamic and pharmacokinetic properties and therapeutic potential in anaemia and the stimulation of erythropoiesis. *Drugs*, 38(6):863–99, 1989.

J. W. Fisher. Erythropoietin: physiologic and pharmacologic aspects. *Proc Soc Exp Biol Med*, 216(3):358–69, 1997.

J. W. Fisher. Erythropoietin: physiology and pharmacology update. *Exp Biol Med (Maywood)*, 228(1):1–14, 2003.

J Gabrielsson and D Weiner. *Pharmacokinetic and Pharmacodynamic Data Analysis: Concepts and Applications*. Swedish Pharmaceutical Press, 4th edition, 2007.

M Gibaldi and D Perrier. *Pharmacokinetics*. Marcel Dekker Inc., New York, 2nd edition, 1982.

John P. Greer, John Foerster, and John N. Luckens. *Wintrobe's Clinical Hematology*. Lippincott Williams & Wilkins, Philadelphia, 11 edition, 2003.

A Groulx. Introduction to pharmacokinetics, 2006.

N. H. Holford and L. B. Sheiner. Understanding the dose-effect relationship: clinical application of pharmacokinetic-pharmacodynamic models. *Clin Pharmacokinet*, 6 (6):429–53, 1981a.

N. H. Holford and L. B. Sheiner. Pharmacokinetic and pharmacodynamic modeling in vivo. *Crit Rev Bioeng*, 5(4):273–322, 1981b.

N. H. Holford and L. B. Sheiner. Kinetics of pharmacologic response. *Pharmacol Ther*, 16(2):143–66, 1982.

W. Jelkmann. The enigma of the metabolic fate of circulating erythropoietin (epo) in view of the pharmacokinetics of the recombinant drugs rhepo and nesp. *Eur J Haematol*, 69(5-6):265–74, 2002.

D. L. Johnson, F. X. Farrell, F. P. Barbone, F. J. McMahon, J. Tullai, K. Hoey, O. Livnah, N. C. Wrighton, S. A. Middleton, D. A. Loughney, E. A. Stura, W. J. Dower, L. S. Mulcahy, I. A. Wilson, and L. K. Jolliffe. Identification of a 13 amino acid peptide mimetic of erythropoietin and description of amino acids critical for the mimetic activity of emp1. *Biochemistry*, 37(11):3699–710, 1998.

M. Kato, H. Kamiyama, A. Okazaki, K. Kumaki, Y. Kato, and Y. Sugiyama. Mechanism for the nonlinear pharmacokinetics of erythropoietin in rats. *J Pharmacol Exp Ther*, 283(2):520–7, 1997.

M. Kato, K. Okano, Y. Sakamoto, K. Miura, T. Uchimura, and K. Saito. Pharmacokinetics and pharmacodynamics of recombinant human erythropoietin in rats. *Arzneimittelforschung*, 51(1):91–5, 2001.

F. Khorasheh, S. Sattari, A. Gerayeli, and A. M. Ahmadi. Application of direct search optimization for pharmacokinetic parameter estimation. *J Pharm Pharm Sci*, 2(3): 92–8, 1999.

C. Kliwinski, D. Makropoulos, D. Kwok, A. Volk, K. Foster, T. Nesspor, C. Huang, and P. Bugelski. Pharmacokinetics and pharmacodynamics of an epo-mimetic fusion protein in a model of chronic renal insufficiency anemia. *Open Hematology Journal*, 4:17–20, 2010.

M. J. Koury, S. T. Sawyer, and S. J. Brandt. New insights into erythropoiesis. *Curr Opin Hematol*, 9(2):93–100, 2002.

S. B. Krantz. Erythropoietin. *Blood*, 77(3):419–34, 1991.

W. Krzyzanski and W. J. Jusko. Mathematical formalism and characteristics of four basic models of indirect pharmacodynamic responses for drug infusions. *J Pharmacokinet Biopharm*, 26(4):385–408, 1998.

W. Krzyzanski, R. Ramakrishnan, and W. J. Jusko. Basic pharmacodynamic models for agents that alter production of natural cells. *J Pharmacokinet Biopharm*, 27 (5):467–89, 1999.

W. Krzyzanski, W. J. Jusko, M. C. Wacholtz, N. Minton, and W. K. Cheung. Pharmacokinetic and pharmacodynamic modeling of recombinant human erythropoietin after multiple subcutaneous doses in healthy subjects. *Eur J Pharm Sci*, 26(3-4): 295–306, 2005.

Lucien Le Cam. Maximum likelihood - an introduction. *ISI Review*, 58(2):153–171, 1990.

G. Levy. Relationship between elimination rate of drugs and rate of decline of their pharmacologic effects. *J Pharm Sci*, 53:342–3, 1964.

O. Livnah, D. L. Johnson, E. A. Stura, F. X. Farrell, F. P. Barbone, Y. You, K. D. Liu, M. A. Goldsmith, W. He, C. D. Krause, S. Pestka, L. K. Jolliffe, and I. A. Wilson. An antagonist peptide-epo receptor complex suggests that receptor dimerization is not sufficient for activation. *Nat Struct Biol*, 5(11):993–1004, 1998.

M. Loeffler, K. Pantel, H. Wulff, and H. E. Wichmann. A mathematical model of erythropoiesis in mice and rats. part 1: Structure of the model. *Cell Tissue Kinet*, 22(1):13–30, 1989.

I. C. Macdougall. An overview of the efficacy and safety of novel erythropoiesis stimulating protein (nesp). *Nephrol Dial Transplant*, 16 Suppl 3:14–21, 2001.

D. E. Mager, E. Wyska, and W. J. Jusko. Diversity of mechanism-based pharmacodynamic models. *Drug Metab Dispos*, 31(5):510–8, 2003.

P. L. Martin, C. Sachs, A. Hoberman, Q. Jiao, and P. J. Bugelski. Effects of cnto 530, an erythropoietin mimetic-igg4 fusion protein, on embryofetal development in rats and rabbits. *Birth Defects Res B Dev Reprod Toxicol*, 89(2):87–96, 2010.

D. N. McLennan, C. J. Porter, G. A. Edwards, A. C. Heatherington, S. W. Martin, and S. A. Charman. The absorption of darbepoetin alfa occurs predominantly via the lymphatics following subcutaneous administration to sheep. *Pharm Res*, 23(9): 2060–6, 2006.

Reza Mehvar. Principles of nonlinear pharmacokinetics. *Am. J. Pharm. Educ.*, 65: 178–184, 2001.

J. J. Perez-Ruixo, H. C. Kimko, A. T. Chow, V. Piotrovsky, W. Krzyzanski, and W. J. Jusko. Population cell life span models for effects of drugs following indirect mechanisms of action. *J Pharmacokinet Pharmacodyn*, 32(5-6):767–93, 2005.

R. Ramakrishnan, W. K. Cheung, F. Farrell, L. Joffee, and W. J. Jusko. Pharmacokinetic and pharmacodynamic modeling of recombinant human erythropoietin after intravenous and subcutaneous dose administration in cynomolgus monkeys. *J Pharmacol Exp Ther*, 306(1):324–31, 2003.

R. Ramakrishnan, W. K. Cheung, M. C. Wacholtz, N. Minton, and W. J. Jusko. Pharmacokinetic and pharmacodynamic modeling of recombinant human erythropoietin after single and multiple doses in healthy volunteers. *J Clin Pharmacol*, 44 (9):991–1002, 2004.

B Reigner, P Jordan, A Panier, and J Glaspy. Cera (continuous erythropoiesis receptor activator), a novel erythropoietic agent: Dose-dependent response in phase i studies. In *Proc Am Soc Clin Oncol 22: 2003 (abstract 2943)*, 2003.

T. D. Richmond, M. Chohan, and D. L. Barber. Turning cells red: signal transduction mediated by erythropoietin. *Trends Cell Biol*, 15(3):146–55, 2005.

P. Sathyanarayana, E. Houde, D. Marshall, A. Volk, D. Makropoulos, C. Emerson, A. Pradeep, P. J. Bugelski, and D. M. Wojchowski. Cnto 530 functions as a potent epo mimetic via unique sustained effects on bone marrow proerythroblast pools. *Blood*, 113(20):4955–62, 2009.

A. Sharma and W. J. Jusko. Characterization of four basic models of indirect pharmacodynamic responses. *J Pharmacokinet Biopharm*, 24(6):611–35, 1996.

L. B. Sheiner. Analysis of pharmacokinetic data using parametric models–1: Regression models. *J Pharmacokinet Biopharm*, 12(1):93–117, 1984.

L. B. Sheiner. Analysis of pharmacokinetic data using parametric models. ii. point estimates of an individual's parameters. *J Pharmacokinet Biopharm*, 13(5):515–40, 1985.

L. B. Sheiner. Analysis of pharmacokinetic data using parametric models. iii. hypothesis tests and confidence intervals. *J Pharmacokinet Biopharm*, 14(5):539–55, 1986.

L. B. Sheiner, D. R. Stanski, S. Vozeh, R. D. Miller, and J. Ham. Simultaneous modeling of pharmacokinetics and pharmacodynamics: application to d-tubocurarine. *Clin Pharmacol Ther*, 25(3):358–71, 1979.

J. L. Spivak. The mechanism of action of erythropoietin. *Int J Cell Cloning*, 4(3): 139–66, 1986.

H. E. Wichmann, M. Loeffler, K. Pantel, and H. Wulff. A mathematical model of erythropoiesis in mice and rats. part 2: Stimulated erythropoiesis. *Cell Tissue Kinet*, 22(1):31–49, 1989.

S. Woo and W. J. Jusko. Interspecies comparisons of pharmacokinetics and pharmacodynamics of recombinant human erythropoietin. *Drug Metab Dispos*, 35(9): 1672–8, 2007.

S. Woo, W. Krzyzanski, and W. J. Jusko. Pharmacokinetic and pharmacodynamic modeling of recombinant human erythropoietin after intravenous and subcutaneous administration in rats. *J Pharmacol Exp Ther*, 319(3):1297–306, 2006.

H. Wu, X. Liu, R. Jaenisch, and H. F. Lodish. Generation of committed erythroid bfu-e and cfu-e progenitors does not require erythropoietin or the erythropoietin receptor. *Cell*, 83(1):59–67, 1995.

H. Wulff, H. E. Wichmann, K. Pantel, and M. Loeffler. A mathematical model of erythropoiesis in mice and rats. part 3: Suppressed erythropoiesis. *Cell Tissue Kinet*, 22(1):51–61, 1989.

Z. Yao, W. Krzyzanski, and W. J. Jusko. Assessment of basic indirect pharmacodynamic response models with physiological limits. *J Pharmacokinet Pharmacodyn*, 33(2):167–93, 2006.

E. Yoshioka, K. Kato, H. Shindo, C. Mitsuoka, S. I. Kitajima, H. Ogata, and T. Misaizu. Pharmacokinetic study of darbepoetin alfa: absorption, distribution, and excretion after a single intravenous and subcutaneous administration to rats. *Xenobiotica*, 37(1):74–90, 2007.

Yong. Zhang, Meirong. Huo, Jianping. Zhou, and Shaofei. Xie. Pksolver: An add-in program for pharmacokinetic and pharmacodynammic data analysis in microsoft excel. *Comput. Methods Programs Biomed.*, 99(3):306–314, 2010.

Appendix A: List of Symbols

AUC	Area under the concentration vs. time curve
$C_{drug}(t)$	Concentration of drug in the central compartment at time t
CL	Clearance: the volume of plasma cleared of the drug per unit time
CL/F	Apparent clearance
C_{max}	Maximum concentration
$C_P(t)$	Concentration of drug in the peripheral compartment at time t
$C(t)$	Concentration of drug in the plasma at time t
EC_{50}	The drug concentration that produces half of the maximum effect
$Ef(t)$	The variable of pharmacological effect
E_{max}	The maximum achievable effect
$E(t)$	Effect function between RET and RBC_M, $E(t)=E_1(t)+E_2(t)$
$E_1(t)$	Effect function from drug concentration
$E_2(t)$	Effect function from change of hemoglobin level
F	Bioavailability: the fraction of drug that is absorbed
$HGB(t)$	Hemoglobin levels at time t

IC_{50}	HGB change for producing 50% maximum inhibition
IIC_{50}	The drug concentration which produces half of maximum inhibitory effect
$II(t)$	Inhibitory function of response
$Input(t)$	Concentration of drug at the s.c. injection site at time t
I_{max}	Maximum inhibition of responses by HGB change.
K_a	Absorption rate
K_{CP}	Inter-compartment exchange rate from central compartment to peripheral compartment
K_e	Output rate constant for $K_{in}(t)$
K_{el}	Elimination rate
K_{in}	The zero-order constant for production of the response
$K_{in}(t)$	Production rate variable for reticulocytes
K_m	The plasma drug concentration at which the elimination rate reaches 50% V_{max} in Michaelis-Menton kinetics
K_{out}	First-order rate constant for loss of the response
K_{out1}	First-order elimination rate of reticulocyte.
K_{out2}	First-order elimination rate of RBC

K_{PC}	Inter-compartment exchange rate from peripheral compartment to central compartment
n	The shape factor in the sigmoid E_{max} model
$RBC(t)$	Red blood cell counts at time t
$RET(t)$	Reticulocyte counts at time t
$R(t)$	The variable for response to a drug
R^2	Coefficient of Determinant
T_d	Delayed time for stimulatory effect and inhibitory effect
T_{RET}	Life span of reticulocyte
SC_{50}	The drug concentration required for producing 50maximum stimulation of $K_{in}(t)$
SSC_{50}	The drug concentration for producing 50% maximum stimulation of response
S_{max}	Maximum stimulation of $K_{in}(t)$ by a drug
SS_{max}	Maximum stimulation of responses by a drug
$SS(t)$	Stimulatory function of response
T_{max}	the time when C_{max} occurs
T_R	Average cell life span

$t_{1/2}$	Elimination half-life
V_C	Volume of distribution at the central compartment
V_d	volume of distribution
V_i	the variance at the ith data point
V_{max}	The maximum elimination rate in Michaelis-Menton kinetics
Y_i	The model predicted value at the ith time point.
λ_z	terminal elimination rate const
σ_{inter}	A parameter of variance model
σ_{slope}	A parameter of variance model

Appendix B: List of Abbreviations

AALAC	American Association for Laboratory Animal Care
AIDS	Acquired immune deficiency syndrome
Baso-EB	Basophilic-erythroblast
BFU-E	Burst forming unit-erythroid
CFU-E	Colony forming unit-erythroid
CV	Coefficient of variation expressed as SD/mean
EPO	Erythropoietin
EPO-R	Erythropoietin Receptor
ESA	Erythropoiesis Stimulating Agent
EMP1	Erythropoietin mimetic peptide-1
HGB	Hemoglobin
HSC	Hematopoietic stem cell
IACUC	Institutional Animal Care and Use Committee
i.m.	Intramuscular
i.v.	Intravenous

MCH	Mean corpuscular hemoglobin
ML	Maximum Likelihood
NCA	Non-compartmental analysis
Ortho-EB	Orthochromic-erythroblast
PD	Pharmacodynamics
PK	Pharmacokinetics
PK/PD	Pharmacokinetic/Pharmacodynamic
Poly-EB	Polychromatophilic-erythroblast
Pro-EB	Proerythroblast
RBC	Red blood cell
RBC_M	Mature red blood cell
RET	Reticulocyte
rHuEPO	Recombinant human erythropoietin
s.c.	Subcutaneous
SD	Standard Deviation
SSE	Sum of square of errors between observations and predicted points
SST	Sum of square of errors from observations to the mean of observations (a horizontal line)

Vita

NAME OF AUTHOR: Wendi Chen

DEGREES AWARDED:

- M.E. in Pattern Recognition and Intelligent Systems, Tsinghua University, 2003
- B.E. in Mechanical and Electronic Engineering, Beijing University of Posts and Telecommunications, 2000

PROFESSIONAL EXPERIENCE:

- Research Assistant in Drexel University, 2005 - 2010
- Teaching Assistant in Drexel University, 2005 - 2010
- Software Engineer in Lucent Technologies, 2003 - 2005

PROFESSIONAL PUBLICATIONS AND REPORT:

- W. Chen, R. Achuthanandam, S. Haney, P. Bugelski, M. Kam and L. Hrebien, "Comparison of Pharmacokinetic/Pharmacodynamic modeling of epoetin-α, darbepoetin-α and CNTO 530 after subcutaneous administration in rats", in submission to *Pharmaceutical Research*.
- W. Chen, R. Achuthanandam, S. Haney, P. Bugelski, M. Kam and L. Hrebien, "A dose threshold study for CNTO 530 after subcutaneous administration in rats", in preparation.

- W. Chen, L. Hrebien, and M. Kam, "Mathematical Modeling of Cell Population Dynamics", *Proc. RISC Day 2007*, Drexel University, April 11, 2007.

- W. Chen, G. Rong and J. Zhou, "Design an Online Signature Verification System for PDA", *Computer Engineering*, Vol. 30, No. 3, p147-149, 2004

- W. Chen, G. Rong and J. Zhou, "An online Chinese Signature Verification System with Continuous Hidden Markov Model", *Proc. of International Conference on Computer, Communication and Control Technologies*, Vol. 1, p205-209, 2003